Report No.
DS-67-7

FINAL REPORT

AGREEMENT NO. FA65 NF-AP-2
PROJECT NO. 520-002-01X

INVESTIGATION OF TURBINE FUEL FLAMMABILITY WITHIN AIRCRAFT FUEL TANKS

by
L. J. NESTOR

JULY 1967

Prepared for

FEDERAL AVIATION ADMINISTRATION
Aircraft Development Service
Engineering and Safety Division
Washington, D. C. 20590

By

NAVAL AIR PROPULSION TEST CENTER
AERONAUTICAL ENGINE DEPARTMENT
Naval Base, Philadelphia, Pa. 19112

GENERAL DISCLAIMER

This document may have problems that one or more of the following disclaimer statements refer to:

- This document has been reproduced from the best copy furnished by the sponsoring agency. It is being released in the interest of making available as much information as possible.
- This document may contain data which exceeds the sheet parameters. It was furnished in this condition by the sponsoring agency and is the best copy available.
- This document may contain tone-on-tone or color graphs, charts and/or pictures which have been reproduced in black and white.
- The document is paginated as submitted by the original source.
- Portions of this document are not fully legible due to the historical nature of some of the material. However, it is the best reproduction available from the original submission.

FINAL REPORT

Project No. 520-002-04X
Report No. DS-67-7

INVESTIGATION OF TURBINE FUEL FLAMMABILITY WITHIN AIRCRAFT FUEL TANKS

JULY 1967

Prepared by

L. J. NESTOR

NAVAL AIR PROPULSION TEST CENTER
AERONAUTICAL ENGINE DEPARTMENT
NAVAL BASE, PHILADELPHIA, PA. 19112

This report has been prepared by the Aeronautical Engine Department of the Naval Air Propulsion Test Center for Aircraft Development Service, Federal Aviation Administration under Agreement No. FA65 NF-AP-2. The contents of this report reflect the view of the department who is responsible for the facts and the accuracy of the data presented herein, and do not necessarily reflect the official views or policy of the FAA. This report does not constitute a standard, specification, or regulation.

FOREWORD

This report was prepared by the Aeronautical Engine Department, Naval Air Propulsion Test Center, for the Federal Aviation Administration. The work effort was part of a program of the Engineering and Safety Division, Aircraft Development Service, Washington, D. C. Engineering liaison and technical review for the project was furnished by the Instruments and Equipment Section, Aircraft Branch, Test and Evaluation Division, National Aviation Facilities Experimental Center, Atlantic City, New Jersey.

ABSTRACT

The equilibrium flammability envelopes of turbine fuels were determined by both visual and instrumental techniques. The lean and rich limits were found to be linear functions of altitude and temperature when wall effects were reduced and ignition spark energies were high. The linearity of the limits could be altered by increasing the wall effects or decreasing the ignition spark energies. Wide-cut turbine engine fuels, aviation kerosenes and blends of the two types were tested. The flammability characteristics of the fuels at equilibrium were compared to those of the fuel under simulated aircraft dynamic conditions. Aircraft dynamics affect fuel primarily by producing spray. When the point of ignition was not directly within the sprayed fuel, no deviation from the normal equilibrium flammability envelope occurred. When the point of ignition was directly within the spray, the lean flammability limit of the fuel was extended considerably beyond the equilibrium limit.

TABLE OF CONTENTS

TABLE OF CONTENTS
(Cont)

LIST OF FIGURES

LIST OF FIGURES
(Cont)

LIST OF FIGURES
(Cont)

LIST OF TABLES

INTRODUCTION

The purpose of this project was to investigate the fuel vapor conditions that exist within aircraft fuel tanks and describe their flammability characteristics. There appears to be an infinite number of conditions that can exist within an aircraft fuel tank. One of the many causes for this complexity is that the inflight conditions which may be experienced by aircraft cover a wide range of temperatures, pressures and motions (1)*. Such broad and extensive environmental conditions produce wide variations in the amount of fuel that exists in the vaporized state. In addition to fuel being present as a vapor, turbulence and aircraft motion cause the liquid to be dispersed in the vapor space in the form of mists and spray. (Mists are distinguished from spray primarily by droplet size and stability of the dispersion. The line of demarcation between the two states is not well defined (2)). Tank characteristics such as design and geometry are contributing factors which produce what amounts to an infinite number of vapor space conditions. Structural members, fuel distribution hardware, quantity gauging equipment, and fuel venting systems all contribute to the complexity of the problem. The fuel sloshes in the tank, spraying fuel into the vapor space; fuel is sprayed into the vapor space by vibration (3) and even by mechanical design such as fuel tank boost pumps which cause jets of fuel to be sprayed into the vapor space (4). Changes in the vapor space composition occur during pressure equilibration of the tank with inflight atmospheric pressures.

Lack of predictability in specifying vapor space fuel/air ratios also results from the fact that the fuels are composed of a rather broad spectrum of compounds with a corresponding broad range of boiling points. During the storage and utilization of the fuel, changing vapor space volumes, and temperature and pressure changes, produce what amounts to a crude form of fractional distillation. The literature abounds with evidence demonstrating that different hydrocarbons show demonstrably different flammability characteristics (5, 6, 7, 8 and 9). Differences in composition, of significant proportions, can exist between fuels, which meet the same specifications but are produced by different refineries or from different crudes (10, 11, 12, and 13).

Further compounding of the problem's complexity occurs from the fact that there are in reality two basically different types of turbine engine fuel that are used by jet aircraft: these are the aviation kerosenes and the wide-cut turbine engine fuels. These fuels are acquired commercially so as to meet either commercial, military or private specifications (1).

* Numbers indicate reference

Any controlled investigation to determine to what degree, any or all combinations of the previously mentioned variables affect fuel/air ratios within tanks necessarily requires an analytical technique and sampling method. To establish a suitable sampling system presents many technical difficulties. For example, it is difficult to see how a sample, representing a specific aerosol and vapor composition can be maintained in its original physical state during transfer until time for analysis. Changes in the physical state of the sample will be produced by temperature gradients, pressure changes, gas flows, and droplet coalescence during sample transfer and final analysis. Also, the location of representative sampling points for a dynamic tank situation, lacking homogeneity, presents a dilemma. The lack of responsiveness and the error that are inherent in a mechanical sampling system would conceivably result in data that could only be suspect. The second alternative for an analytical scheme would be one which does not require any sampling. For such an approach to defining the liquid-vapor state an optical system would appear most practical. Such an insitu optical display has the advantage of not altering the liquid-vapor states, but a decided disadvantage exists with respect to its describing an aerosol. No satisfactory analysis of a polydisperse cloud, be it a mist or spray, can be made either by scattered light, transmitted light, variation in the color of the scattered light or its polarization (2). From the arguments presented, it is easy to see that a program which is designed along analytical principles to define liquid-vapor conditions of an aircraft fuel tank and their flammability is beyond practical considerations. Therefore, this investigation was carried out on the basis of defining actual flammability in terms of the environmental conditions to which an aircraft fuel tank might be exposed. An experimental combustion apparatus was designed which made this possible. The apparatus contained the liquid fuel within the combustion chamber at all times. Therefore, any change in environmental conditions could be related directly in terms of variations to the natural limits of flammability.

This report describes the equilibrium flammability characteristics of two types of turbine engine fuels, in terms of altitudes and temperatures. The effects on flammability of simulated ground storage, aircraft flight conditioning and blends of an aviation kerosene with a wide-cut turbine engine fuel are included.

In addition to the conventional definition of flammability using the visual confirmation of flames, the flammability characteristics of fuels were investigated in terms of transient pressure and temperature rises which were produced upon igniting a tank vapor space. These pressure and temperature rises made possible the means by which the effect of fuel spray was evaluated. The flammability data on

the spray provided insight into the relative flammability characteristics within an aircraft tank under static and dynamic conditions. By the further application of instrumental techniques, flammability studies included venting out of tanks during aircraft ascent. Combustion data were obtained during conditions which simulated aircraft takeoff and ensuing climb.

DISCUSSION

Physical Properties of Fuels and Their Relationship to Fuel Flammability

Turbine engine fuels are rather complex blends of a variety of hydrocarbons, i.e. paraffins, olefins, aromatics and naphthenics. For example, it is reported that some 5,000 to 10,000 hydrocarbons are contained in JP-4 jet fuel (14). A narrower boiling range fuel such as gasoline has some 300 individual hydrocarbons. Because of the chemical complexity of fuels, they are classified on the basis of their physical properties. Turbine engine fuels are placed in two broad categories, which are based on their distillation temperature ranges: wide-cut turbine engine fuels and aviation kerosenes (1). These in turn are purchased operationally according to a variety of specifications-military, consumer organization, airline and engine manufacturer (15). Primarily, the differences between any of these fuels are due to the relative proportions of the hydrocarbon constituents. Various specifications of turbine fuels are shown in Tables I and II. Although many other specifications exist, the ones shown here are those which are commonly used and are pertinent to this report.

1. Fuel Volatility - Combustion is primarily a process involving vapors. For example, in the burning of a fuel droplet, three distinct phases occur (16). In the first stage the droplet is preheated to a point where sufficient vapors are evolved to support a flame. In the second stage, the heat from the enveloping flame causes fuel vapors to evolve continuously and feed the flame. In the final stage, the combustion of a cokelike residue may occur. Fuel volatility, therefore, is one of the primary characteristics that relate to fuel flammability. Those specification properties which are a measure of volatility are: flash point, distillation range and vapor pressure. These are the primary properties that are inferred when differences in flammability are claimed for one fuel in comparison with another (1).

TABLE I

UNITED STATES MILITARY SPECIFICATION FOR AVIATION TURBINE FUELS

Specification:	- - - - MIL-T-5624G (Amend. 1) - - - -	
Effective Date:	- - - - - - - - -11/21/66- - - - - - - -	
Grade:	JP-4	JP-5
Type:	Wide-Cut	Kerosene
Distillation:		
Initial boiling point	(a)	(a)
Fuel evaporated, 10 percent min. at	(a)	400°F (204.4°C)
Fuel evaporated, 20 percent min. at	290°F (143.3°C)	(a)
Fuel evaporated, 50 percent min. at	370°F (187.8°C)	(a)
Fuel evaporated, 90 percent min. at	470°F (243.3°C)	(a)
End point, max.	(a)	550°F (287.8°C)
Percent evaporated, at 400°F (204.4°C)	(a)	- - -
Residue, vol. percent max.	1½	1½
Distillation loss, vol. percent max.	1½	1½
Gravity °API - min. (sp. gr. max.)	45.0 (0.802)	36.0 (0.845)
Gravity °API - max. (sp. gr. min.)	57.0 (0.751)	48.0 (0.788)
Existent gum, mg./100 ml. max.	7	7
Total potential residue, 16 hour aging, mg./100 ml. max.	14	14
Sulfur, total, percent weight max.	0.4	0.4
Mercaptan sulfur, percent weight max. (b)	0.001	0.001
Reid vapor pressure, 100°F, psi, min., ($gm./cm^2$, min.)	2.0 (140.6)	- - -
Reid vapor pressure, 100°F, psi, max., ($gm./cm^2$), max.)	3.0 (210.9)	- - -
Freezing point, max.	-72°F (-58°C)	-51°F (-46°C)
Heating Value:		
Net heat of combustion, Btu/lb., min., or aniline-gravity product, min. (c)	18,400 5,250	18,300 4,500
Viscosity, centistokes at -30°F (-34.4°C), max.	- - -	16.5
Aromatics, vol. percent max.	25.0	25.0
Olefin, vol. percent max.	5.0	5.0
Smoke point, mm. min.	- - -	19.0
or luminometer No., min.	- - -	50
Explosiveness, percent max.	- - -	50
Flash point, min.	- - -	140°F (60.0°C)
Smoke volatility index, min.	52.0 (d)	- - -
or luminometer No., min.	60	- - -
Copper strip corrosion, ASTM classification max.	No. 1	No. 1
Water separometer index, modified min.	70	85
Water reaction, interface rating, max.	1 b	- - -
Thermal stability:		
Change in pressure drop in 5 hours, in. of Hg., max.	3.0	3.0
Preheater deposit code, less than	3	3
Particulate matter,		
mg./gal. max. F.O.B. origin deliveries	4.0	- - -
mg./gal. max. F.O.B. destination deliveries	8.0	- - -
Fuel system icing inhibitor, percent vol., max.	0.15	- - -
Fuel system icing inhibitor, percent vol., min.	0.10	- - -

(a) To be reported - not limited.

(b) The mercaptan sulfur determination may be waived at the option of the inspector if the fuel is "doctor sweet" when tested in accordance with Method 5203 of Federal Test Method Standard No. 791.

(c) Aniline-gravity product is defined as the product of the gravity in °API and the aniline point in °F.

(d) The smoke volatility index (SVI) is the smoke point (SP) + (0.42 X volume percent boiling under 400°F (204.4°C)).

TABLE II (Ref. 15)

COMMERCIAL SPECIFICATIONS FOR AVIATION TURBINE FUELS

Organization:		ASTM		
Grade:		Jet A	Jet A-1	Jet B
Effective Date:			1966	
Type:		Kerosene	Kerosene	Wide-Cut
Gravity, °API Min. (Sp. Gr. Max.)			39 (0.8299)	45 (0.8017)
Gravity, °API Max. (Sp. Gr. Min.)			51 (0.7753)	57 (0.7507)
Distillation, °F (°C)				
10% Evaporated			400 (204.4) Max.	- - - -
20% Evaporated			- - - -	290 (143.3) Max.
50% Evaporated			450 (232.2) Max.	370 (187.8) Max.
90% Evaporated			- - - -	470 (243.3) Max.
Final Boiling Point			550 (287.8) Max.	- - - -
Residue, Vol. %			1.5 Max.	1.5 Max.
Loss, Vol. %		S	1.5 Max.	1.5 Max.
Flash Point, °F (°C) Min.		A	110 (43.3)	- - - -
Flash Point, °F (°C) Max.		M	150 (65.6)	- - - -
Reid Vapor Pressure, psi		E	- - - -	3 Max.
Aromatics, Vol. %		A	20 Max.	20 Max.
Olefins, Vol. %		S	- - - -	5 Max.
Sulfur, Total, Wt. %			0.3 Max.	0.3 Max.
Mercaptan Sulfur, Wt. %		J	0.003 Max.	0.003 Max.
or Doctor Test		E	Pass	Pass
Total Acidity, mg KOH/gm		T	0.1 Max.	- - - -
Copper Strip Corrosion		A-1		
3 Hours at 122°F (50°C)			No. 1 Max.	- - - -
2 Hours at 212°F (100°C)			- - - -	No. 1 Max.
Existent Gum, mg/100 ml			7 Max.	7 Max.
Total Potential Residue				
16 Hour Test, mg/100 ml			14 Max.	14 Max.
Thermal Stability 300/400°F (148.9/204.4°C)				
ΔP (5 Hours at 6 lb/hr), Inches Hg			12 Max	12 Max.
Preheater Tube Deposit			<3	<3
Freezing Point °F (°C)		-36 (-38) Max.	-54 (-48) Max.	-56 (-49) Max.
Viscosity at -30°F (-34.4°C), cs			15 Max.	- - - -
Heat of Combustion, Net BTU/lb			18,400 Min.	18,400 Min.
or Aniline-Gravity Product			- - - -	- - - -
Heat of Combustion, Net BTU/gal			Report	Report
Combustion Properties - Must Pass One:				
1. Luminometer Number		S	45 Min.	50 Min.
2. Smoke Point, mm		A	25 Min.	- - - -
3. Smoke Point, mm		M	20 Min.	- - - -
and 16 Hour Lamp Burning Test		E	Pass	- - - -
4. Smoke Point, mm			20 Min.	- - - -
and Naphthalenes, Vol. %		A	3 Max.	- - - -
5. Smoke Volatility Index (a)		S	- - - -	54 Min.
Water Tolerance, Vol. Change, ml		J	±1	±1
Interface Rating		E	- - - -	- - - -
Electrical Conductivity		T		
Picomho/meter at Delivery Temp.			- - - -	- - - -
Additives		A-1		
Antioxidant			By agreement between vendor and purchaser	
Metal Deactivator				
Corrosion Inhibitor				
Anti-Icing				
Anti-Static				

(a) Smoke Volatility Index (SVI) = Smoke Point + 0.42 (Vol. % Evaporated at 400°F (204.4°C))

2. Flash Point - The flash point which is normally determined only for the aviation kerosenes, is an estimate of the minimum temperature at which sufficient vapor is released by the fuel to form a flammable vapor-air environment at one atmosphere pressure. For pure hydrocarbons, such as n-alkanes, flash point data have been successfully correlated with lean flammability limits as well as vapor pressures (17). However, because of experimental errors, apparatus effects and fuel fractionation, flash point data for turbine engine fuels lose a good deal of their fundamental significance. The usefulness of flash points with respect to turbine engine fuels should be limited to establishing relatively large flammability differences between fuels.

A comparison of some flash point data obtained by the Pensky-Martin closed cup method, with the lean flammability limits, determined in this investigation, confirms that, although flash points do provide a satisfactory method for approximating lean flammability limits of pure materials, they fail to give a good correlation for turbine engine fuels. This is shown in Table III.

TABLE III

COMPARISON OF FLASH POINT DATA WITH THE LEAN FLAMMABILITY LIMITS OF HEXANE AND TURBINE FUELS

Fuel	Flash Point, °F (Pensky-Martin Closed Cup)	Lean Flammability Limit, °F	Difference °F
Hexane	-23 (17)	-17	+6
Jet A	125	98	-27
Jet A-1 (Batch 1)	120	101	-19
Jet A-1 (Batch 2)	118	92	-26
Jet B (Batch 2)	<-30 *	-20	>10
Jet B (Batch 3)	<-30 *	-8	>22

* adaptation

3. Distillation Range - The distillation ranges of the fuels reported during these investigations are included in Appendix I along with the results of the other pertinent specification tests.

The exact behavior of multiple component systems such as turbine engine fuels defies description. Nevertheless, by mere inspection of the data in Appendix I, the lower and the relatively broader distillation ranges of the wide-cut turbine engine fuels demonstrates that they have a considerably greater proportion and variety of light ends, i.e. low molecular weight and high vapor pressure hydrocarbons, than the aviation kerosenes.

Aside from this qualitative insight, the distillation data are useful for calculating the vapor pressures of these fuels. For example, Zengel, et al, reports a method for calculating vapor pressures, on the basis of distillation data, with a precision claimed to be within ±5 percent (18). Difficulty is usually met however, in obtaining suitably accurate distillation data, especially for the lower boiling point components. Distillation data, of the type normally obtained for specification requirements, are used for calculating the equilibrium combustibility envelopes of turbine engine fuels.

4. Vapor Pressures - Vapor pressure affects flammability by controlling the amount of fuel in the vapor space. In a fuel tank which is only partially filled with fuel, the fuel molecules escape from the liquid into the space above it. If it is a closed vessel, the space is limited and the molecules will steadily accumulate in the vapor space. As the number of molecules increase in the space, the number of molecules returning to the liquid increases accordingly. If the temperature is maintained constant, a condition of equilibrium becomes established when the number of molecules leaving the liquid equals the number of molecules returning. The pressure which the liquid molecules exert in the vapor space is the vapor pressure. In theory, then, it becomes apparent that knowing the vapor pressure at a particular temperature for a closed system, and knowing the volume of the available vapor space (ullage), a fairly accurate estimate of the amount of fuel existing as a vapor can be made, provided of course that the liquid and gas behave in an ideal manner. However, the vapor pressure data that are generally available from specification testing are the Reid vapor pressures, which are usually reported only for the higher vapor pressure, wide-cut turbine engine fuels. The Reid vapor pressure data suffer with respect to their usefulness in calculating flammability limits since they represent vapor pressures only at a temperature of 100°F. In order to calculate flammability limits, the vapor pressures of the fuel must be available for an extended temperature range.

Equilibrium Flammability Characteristics of Turbine Fuels

1. Description of the Equilibrium Flammability Envelope - A closed tank, which is only partially filled with fuel, and kept at a constant temperature, would eventually form an equilibrium condition between fuel and vapor. By definition, equilibrium and maximum fuel/air ratio are synonomous. Because of this natural limitation, equilibruim is the basis for all experimentation since it is not only reproducible but is also applicable to theoretical and thermodynamic treatments.

The vapor space in a fuel tank varies in its flammability according to the concentration of evaporated fuel in the available air. Reducing the fuel to air ratio below a definite minimum value produces a vapor space mixture which is too lean in fuel to burn. Likewise, there is a limiting maximum fuel/air ratio, which when exceeded, results in a vapor space mixture too rich in fuel to be flammable. When considering only equilibrium conditions, the particular fuel/air ratio which can exist is determined by the temperature and pressure of the system. The temperature determines the quantity of the fuel by controlling its vapor pressure, and the altitude determines the quantity of air. Therefore, by a suitable combination of temperature and altitude, under equilibrium conditions, the ullage of a fuel tank can be made either flammable or nonflammable.

The environmental parameters of temperature and altitude which will affect the flammability of the tank ullage, are illustrated by the use of the "flammability envelope". A typical flammability envelope is shown in figure 1.

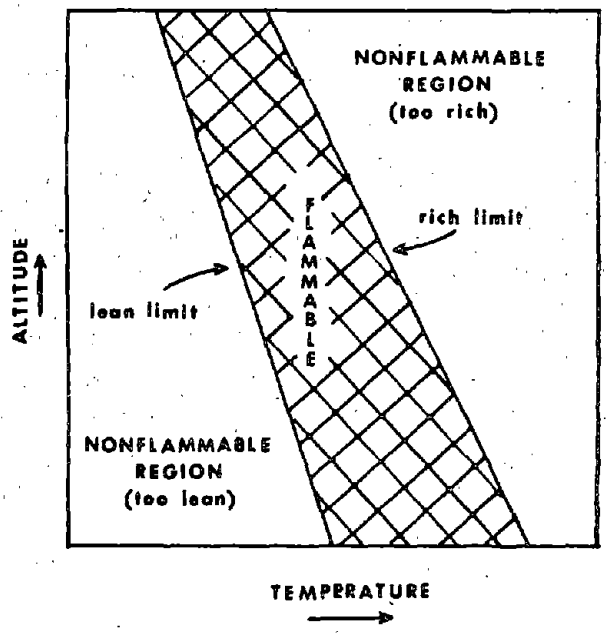

Figure 1 - Typical Flammability Envelope of an Aircraft Turbine Fuel

For aircraft turbine fuels, the lean limit fuel/air ratio is reported to be approximately 0.035 (14). The rich limit designates the maximum fuel/air ratio that is flammable. For aircraft turbine fuels, the rich limit fuel/air ratio is reported to be approximately 0.26 to 0.28 (14). For calculation purposes, the 0.28 value was used in this investigation.

Extreme changes in temperature moderately affect the fuel/air ratios representing flammability limits. For example, based upon data reported by Zabetakis (6), the lean limit fuel/air ratio of methane is 0.033 at 77°F and 0.035 at 212°F. The rich limit fuel/air ratio of methane is 0.102 at 77°F and 0.107 at 212°F. The limiting values are also not affected significantly by changes in pressure. Therefore, when considering the temperature and pressure ranges which are applicable to the environmental conditions encountered by commercial aircraft, the limiting fuel/air ratios can be assumed to be relatively constant. The reasonableness in treating the limiting fuel/air ratios as being constant is further supported by the fact that the fuel/air ratios, which were referenced previously, are only average values. It is probably true that the variations in the limiting fuel/air ratios which result from compositional difference between fuels is far greater than any deviation produced by the temperature and pressure variations of flight. Taking these factors into account, we may treat the lean flammability limit and rich flammability limit as lines which designate constant fuel/air ratios, and are respectively 0.035 and 0.28.

The equilibrium flammability envelopes can be altered by a number of variables. A listing of some of these variables is as follows:

a. Nature of Aircraft Turbine Fuels

(1) Varying flammability limit fuel/air envelopes which are characteristic of the predominant hydrocarbons present in the fuel fraction that has been vaporized.

(2) Variable vapor pressures.

(3) Changing character of the liquid fuel caused by evaporation of light ends.

b. Mechanical Effects

(1) Tank or chamber design and geometry.

(2) Wall effects which can modify combustion reactions.

(3) Intensity and nature of ignition source.

(4) Mechanical spraying of fuel such as by tank boost pumps.

c. Flight Environmental Effects

(1) Altitude changes.

(2) Temperature changes.

(3) Variable ullage.

(4) Tank venting.

(5) Spraying of fuel by the agitation due to aircraft motion.

(6) Mixing of fuels as during refueling operations.

d. Definition of a Flame - The exact temperatures and pressures which are designated by a particular flammability envelope depend upon the investigator's definition of a flame. Such a definition may be based upon arbitrary subjective characteristics or instrumental parameters.

2. Experimental Equilibrium Flammability Envelopes as Determined by the Visual Method - The classical approach for defining flammability limits of gases in a closed system when using electrical spark ignition, involves the use of a glass tube combustion apparatus, and visually confirming a resultant flame upon spark ignition. Zabetakis defined a flammable fuel/air ratio as one where the flame propagation is essentially independent of the ignition source. This characteristic is established by the ability of the flame to traverse a minimum distance of four feet along the tube (5, 6). A nonflame, in this report, is defined as one where no visual confirmation of a flame could be made, or the flame failed to propagate the minimum distance of four feet.

A glass tube apparatus and techniques were developed to establish flammability envelopes especially for aircraft turbine fuels. A detailed description of this apparatus and experimental procedure is given in Appendix II, "Glass Tube Combustion Apparatus".

The distinguishing feature of this particular combustion apparatus, which made it applicable to fuels, is that the fuel sample was retained in the combustion apparatus throughout the entire experimental procedure, including ignition. This design feature made possible the formation of the natural equilibrium fuel/air ratios from the liquid fuel, and avoided the difficulties involved in preparing valid mixtures of air and vaporized fuel components.

The combustion apparatus, which was used for determining the equilibrium flammability envelopes, had incorporated in its design certain characteristics that minimized the apparatus effects which distort the flammability envelopes. These characteristics are described in Appendix IV. The suitability of the glass tube apparatus, ignition system and techniques were confirmed by determining experimental equilibrium flammability limits for n-hexane (Appendix IV) and comparing these data with the theoretical values and limits that were established by other investigators. This comparison of the n-hexane data is made in Table XII of Appendix IV.

The basic procedure employed throughout the glass tube combustion experiments involved the introduction of a constant volume fuel sample into the combustion apparatus. Before the introduction of fuel sample, the apparatus was evacuated to a vacuum of 29 to 29.5 inches of mercury and made completely void of fuel vapor by a constant air purge. The volume of fuel was standardized to produce a ullage of 87.5%. The apparatus was maintained at the desired experimental temperature throughout this procedure.

The flammability envelopes were determined graphically, selecting a line beyond which no experimental flammable points were observed. This method for establishing the limit was selected on the basis that it provided a conservative representation of a flammability limit. This characterization of a limit differs from that of some other investigators who define a limit as the limiting mixture composition between flammable and nonflammable mixtures (6). Application of this latter definition on a statistical basis may result in flammability limits with a random scatter of flammable points about the line. Although technically correct this inherent scatter shows flammable points in nonflammable regions of the envelope. Therefore by using the former designated graphical technique, this apparent anomaly was avoided. In either case, however, the differences between the types of limits, depending upon the definition, were only minor. The limits determined by averaging points between a flame and nonflame would be located approximately 5°F within the envelope as compared with the limits which were graphically located to restrict flammable points within the flammability envelope.

The flammability envelopes of the aviation kerosene type fuels (Jet A, figure 2, and Jet A-1, figure 3), differ from the wide-cut turbine engine fuels (JP-4, figure 4, and Jet B, figures 5 and 6), primarily in their temperature ranges. From Table IV, which summarizes the equilibrium flammability data, the aviation kerosenes have an average experimental lean limit at sea level of about 100°F and a rich limit of approximately 180°F. (Data of two of the fuels shown are not included in figures 2 through 6.) For the wide-cut turbine engine fuels, the lean and rich limits at sea level are about -10°F and 50°F, respectively. The slopes of the lean limits, for either fuel, generally showed a higher rise in altitude for each degree Fahrenheit reduction in temperature than did the rich limit slopes.

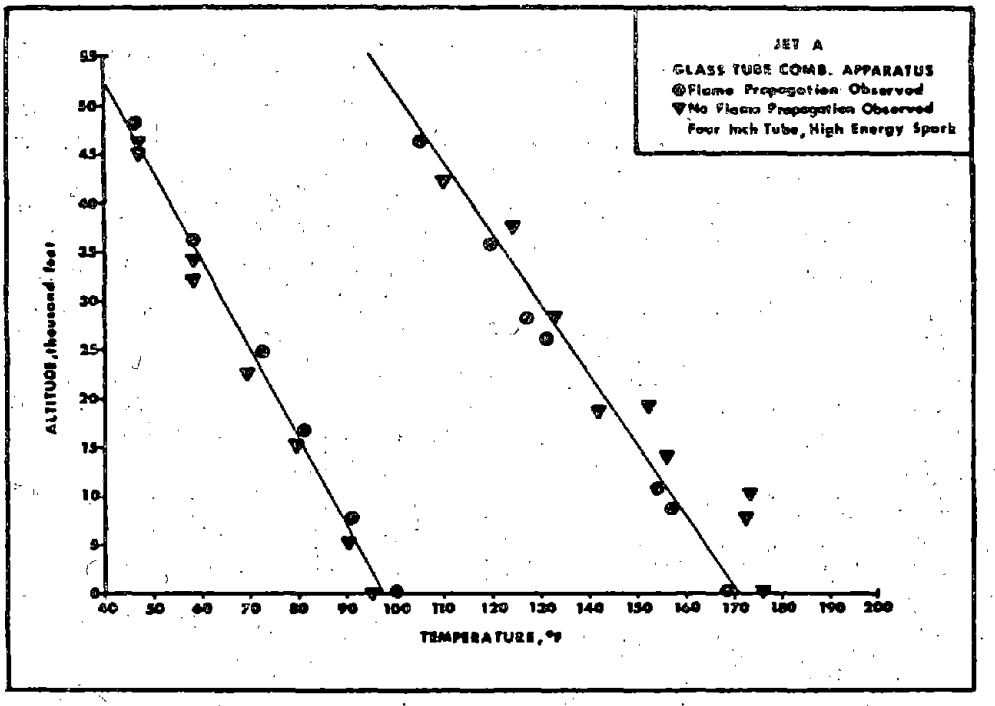

Figure 2 - Equilibrium Flammability Envelope of Jet A

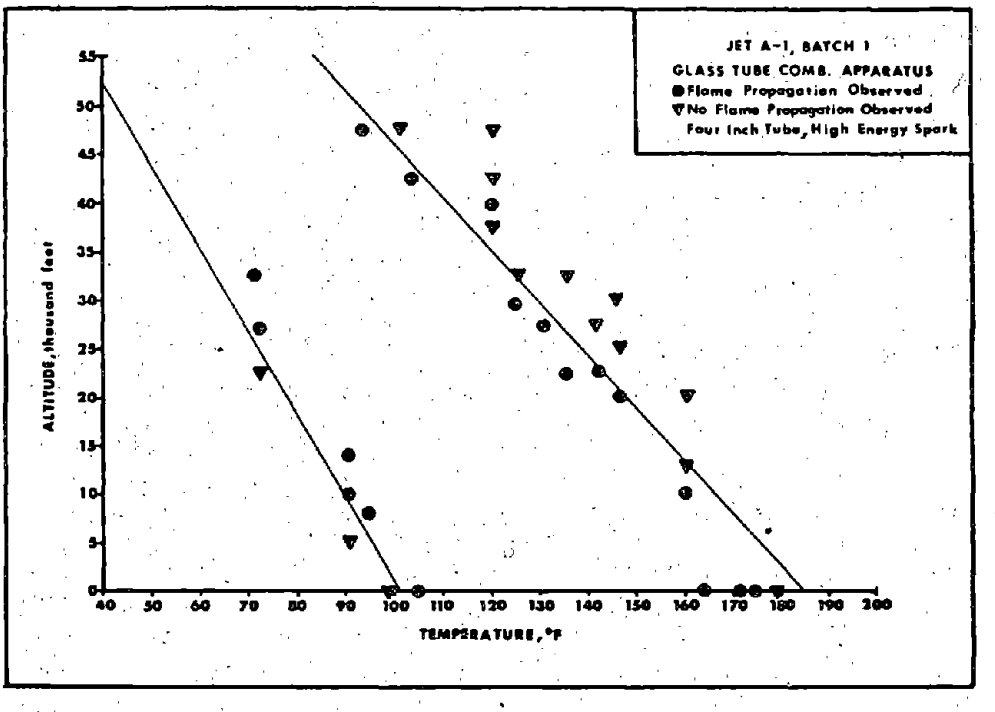

Figure 3 - Equilibrium Flammability Envelope of Jet A-1

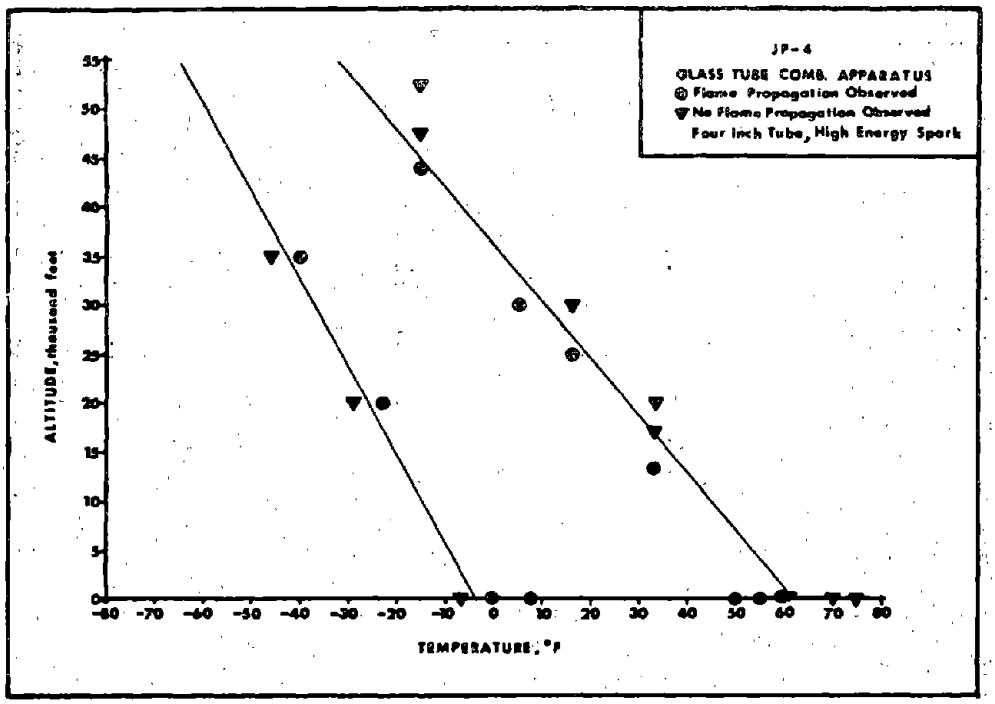

Figure 4 - Equilibrium Flammability Envelope of JP-4

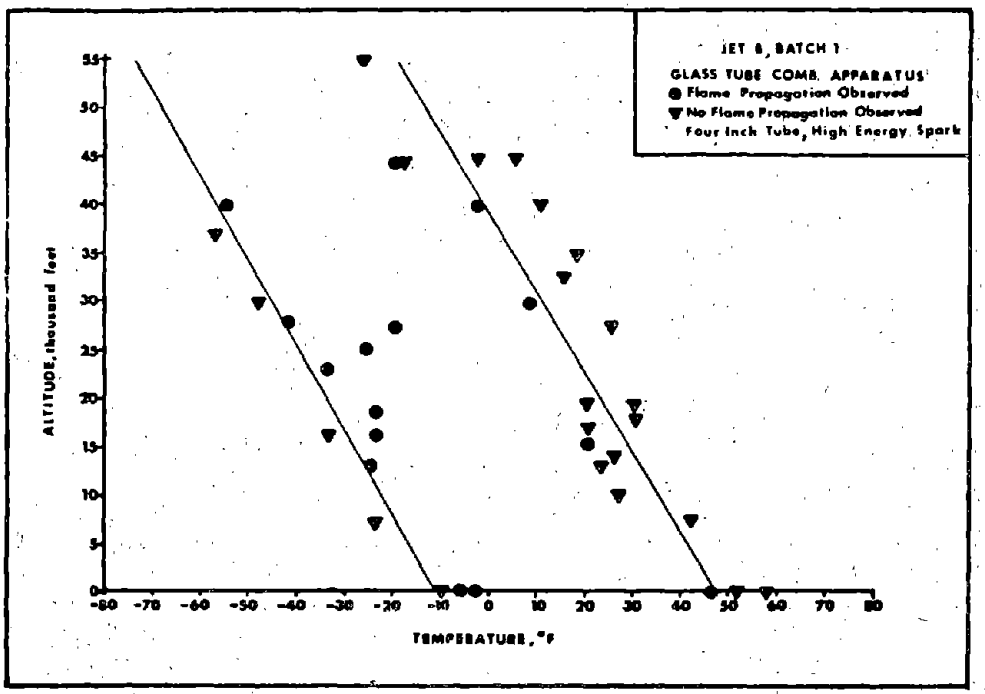

Figure 5 - Equilibrium Flammability Envelope of Jet B, Batch 1

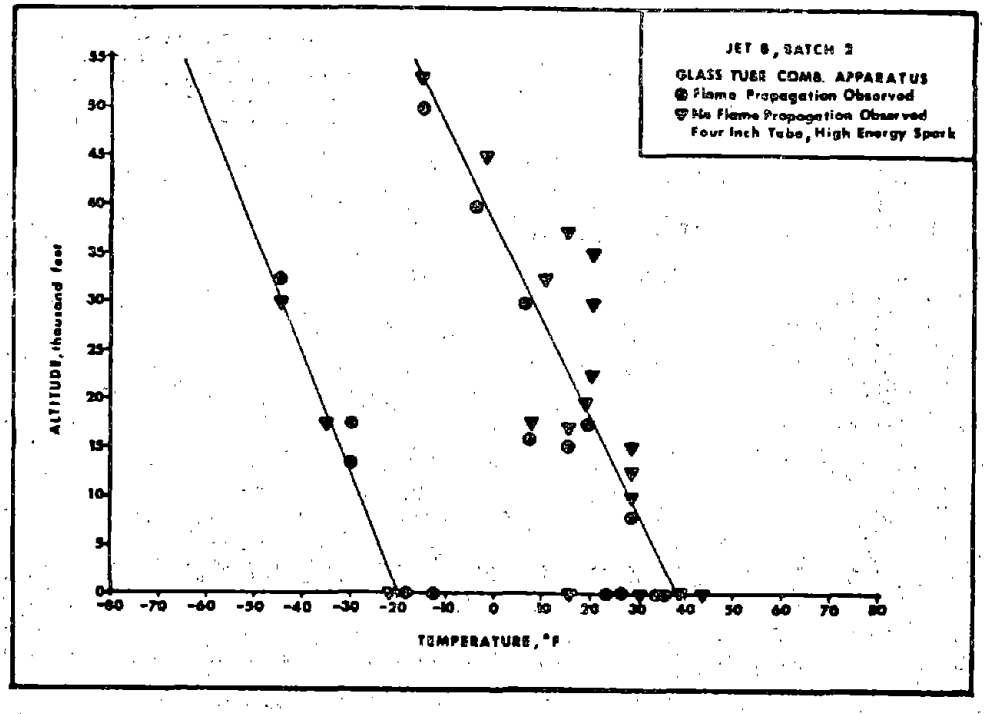

Figure 6 - Equilibrium Flammability Envelope of Jet B, Batch 2

3. Calculated Flammability Limits - The method for calculating flammability limits of turbine fuels is described in Appendix V. Using this method the flammability limits were calculated for four samples of wide-cut turbine fuels and three samples of aviation kerosenes. The results are shown in Table IV, along with the experimental data for the same fuels. This table shows that agreement between calculated and experimental results varies from quite good to poor. The kerosene flammability limits appear to be more amenable to satisfactory calculation by the method used than are the wide-cut fuels.

There are several potential sources of error which may lead to these differences in results. Several generalizations are made in utilizing, for heterogeneous fuels, equations which are derived for use with pure compounds. The normal boiling point, entropy of vaporization and molecular weight of the vapors are estimated by empirical relationships with the A.S.T.M. distillation characteristics of the fuels. These specific relationships are not necessarily valid for all fuel samples, especially among the wide-cut fuels, and the distillation method used is not as precise as could be desired.

TABLE IV

CALCULATED FLAMMABILITY LIMITS OF TURBINE FUELS

		Lean Limit, °F			Rich Limit, °F		
	Altitude (Ft.)	Calculated (a)	Experimental (c)	Error (d)	Calculated (b)	Experimental (c)	Error (d)
WIDE-CUT TURBINE ENGINE FUELS							
JP-4	Sea Level	10	-4	14	75	63	12
	40,000	-32	-48	16	19	-6	25
Jet B, Batch 1	Sea Level	5	-11	16	69	48	21
	40,000	-36	-57	21	14	-1	15
Jet B, Batch 2	Sea Level	6	-20	26	71	38	33
	40,000	-35	-53	18	15	-2	17
Jet B, Batch 3	Sea Level	14	-8 (e)	22	79	56 (e)	23
	40,000	-28	-55 (e)	27	23	-8 (e)	31
		Average Error		20			22
AVIATION KEROSENES							
Jet A	Sea Level	111	97	14	186	172	14
	40,000	60	53	7	123	116	7
Jet A-1, Batch 1	Sea Level	111	100	11	186	185	1
	40,000	60	54	6	123	111	12
Jet A-1, Batch 2	Sea Level	106	89 (e)	17	181	184 (e)	-3
	40,000	59	41 (e)	18	118	102 (e)	12
		Average Error		12			7

(a) Based on fuel/air ratio of 0.035 (wt.)

(b) Based on fuel/air ratio of 0.28 (wt.)

(c) Glass tube combustion apparatus.

(d) Calculated minus the experimental value.

(e) Dynamic combustion apparatus.

Another source of error may be in the use of standard or average values for the lean and rich flammability limit fuel/air ratios. There is significant variation in these parameters among pure hydrocarbons as shown in Table V. The actual vapor composition in tanks containing turbine fuels is unknown and is certain to vary significantly among various types of fuel and at various temperatures. Therefore it is quite possible that the flammability limit fuel/air ratios for the vapors may be different from the standard ratios. As the method must assume standard values to be applicable to all fuels, errors are unavoidable.

TABLE V

LIMITING FUEL/AIR RATIOS OF PARAFFINIC HYDROCARBONS

	Lean Limit		Rich Limit	
	Vol. Percent (Ref. 6)	Wt. Ratio	Vol. Percent (Ref. 6)	Wt. Ratio
methane	5.0	.029	15.0	.098
ethane	3.0	.032	12.4	.147
propane	2.1	.033	9.5	.160
n-butane	1.8	.037	8.4	.184
n-pentane	1.4	.035	7.8	.211
n-hexane	1.2	.036	7.4	.238
n-heptane	1.05	.037	6.7	.249

The effect of errors in the fuel/air ratio can be seen by calculating the limits for a fuel for which the flammability limit fuel/air ratio is well known. Table VI shows these values for n-hexane, a pure hydrocarbon compound which has been thoroughly investigated experimentally. The equilibrium lean and rich limits in terms of temperature are shown as calculated from the standard "average" fuel/air ratios used in this report, and from the actual limit fuel/air ratios. These limits are compared to those obtained experimentally in this program using the four-inch diameter glass tube with high energy spark. There is appreciably better agreement when the actual fuel/air ratios are used.

TABLE VI

CALCULATED FLAMMABILITY LIMITS OF n-HEXANE

Altitude (Ft.)	Fuel/Air Ratio, Wt.	Lean Limit, °F Calculated	Experimental (a)	Error (b)
Sea Level	.035 (c)	-18	-17	-1
40,000	.035 (c)	-57	-59	2
Sea Level	.0361 (d)	-17	-17	0
40,000	.0361 (d)	-56	-59	3
		Rich Limit, °F		
Sea Level	0.28 (c)	44	36	8
40,000	0.28 (c)	-8	-19	11
Sea Level	.238 (d)	38	36	2
40,000	.238 (d)	-13	-19	6

(a) 4-inch diameter glass tube apparatus
(b) Calculated minus the experimental value
(c) Average fuel/air ratio (14)
(d) Experimental derived fuel/air ratios (6)

Effect of the Fuel's Prior History on the Equilibrium Flammability Envelopes

1. Storage - The fuels, Jet A and Jet B, were stored for four months in a vented tank at ambient pressures and temperatures. The temperature fluctuations were moderate, occurring within the narrow range of 70±15°F. At the conclusion of this four-month storage period, flammability envelopes were determined using the four-inch glass tube combustion apparatus and the high energy, 20 joule, a.c. spark. The resultant flammability envelopes are shown in figures 7 and 8 which also include the envelopes of the fuels prior to storage.

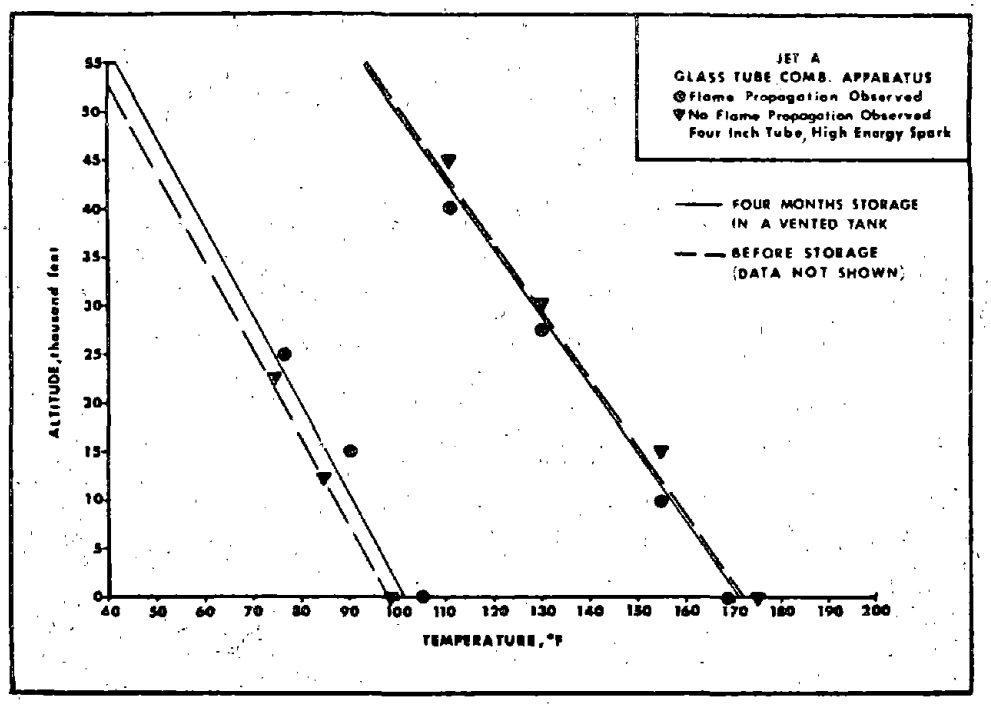

Figure 7 - Effect of Four Months' Storage on Jet A-1

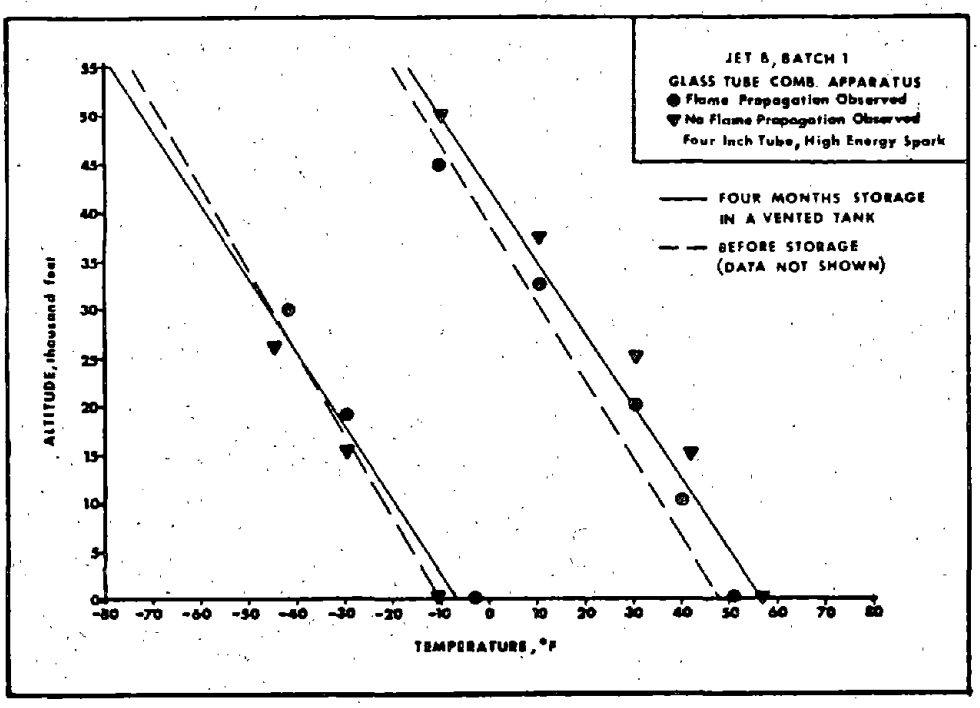

Figure 8 - Effect of Four Months' Storage on Jet B

The envelopes for the stored fuels are almost identical to the envelopes representing the original fuels. The minor deviations in the slopes and intercepts of the limit lines are considered to be within the repeatability of the determination and are therefore not significant.

2. Flight Conditioning - Unused fuel remaining in an aircraft is fuel which may have been exposed to some extreme environmental conditions. It is the purpose of this phase of the investigation to determine if fuel, exposed to a simulated flight cycle (takeoff-ascent-continued flight-descent-landing, etc.) would deviate from its normal flammability envelope. Flight conditioned fuel, as referred to in this report, is fuel which had been weathered by a series of pressure fluctuations to simulate a hypothetical flight profile. This hypothetical flight profile is described in Table VII. Flight conditioning involved only the pressure changes associated with the respective altitudes. No attempt was made to vary the temperature of the fuels to simulate temperature variations which would occur at these altitudes. With the fuel remaining at room temperature, the severity of the flight conditioning treatment could be considered greater than would occur in actual flight during which the colder temperatures at altitude would tend to reduce evaporation losses. Table VIII lists the experimentally determined flammability limits for both the normal and flight conditioned Jet A-1 and Jet B fuels. The limits shown are at the altitudes of 0, 20,000 and 30,000 ft. A comparison of the limits for the Jet A-1 fuel indicates that in spite of the severity of the flight conditioning treatment, no significant changes were produced. However, the flight conditioning of the more volatile Jet B altered the slope of the rich limit from 1000 ft. to 2000 ft. per °F. The equilibrium flammability limits of the flight conditioned Jet B at sea level were similar to those of the normal fuel. The differences between the limits of the two fuels increase with increasing altitudes. Therefore, although the data are limited, they suggest that flight conditioning has little effect on the less volatile aviation kerosenes, and increases the slopes of the limits for the more volatile, wide-cut turbine engine fuels.

3. Fuel Mixing - Because the availability of the various type fuels differs with location, mixing of fuels in aircraft fuel tanks is conceivable (1). An aircraft tank, partially filled with the unused portion of one type of fuel, may be refueled with another. Thus, for example, Jet A may be intermixed with Jet B in all possible proportions. To establish what effects this mixing might have on the flammability of the blended fuel, intermediate blend formulations were prepared and their equilibrium flammability characteristics were determined.

TABLE VII

HYPOTHETICAL FLIGHT PROFILE ADOPTED FOR "FLIGHT CONDITIONING" FUEL

Volume of Fuel: 5 gallons Volume of Tank: 20 gallons
Temperature: 80° to 90°F

Step	Initial Altitude, thousand feet	Final Altitude, thousand feet	Rate of Ascent, thousand feet per minute	Time Duration at Final Altitude, Hours
1	0	40	10	2
2	40	0	-	¼
3	0	10	2	1
4	10	0	-	¼
5	0	40	5	2
6	40	0	-	¼
7	0	40	10	1
8	40	0	-	End of Conditioning

TABLE VIII

FLAMMABILITY LIMITS OF "FLIGHT CONDITIONED" FUELS

Altitude, thousand feet	Lean Limit Temp., °F		Rich Limit Temp., °F	
	Normal Fuel	Conditioned Fuel	Normal Fuel	Conditioned Fuel
	JET B, BATCH 2			
0	-20	-19	38	38
20	-36	-32	18	27
35	-49	-	3	17
	JET A-1, BATCH 1			
0	100	94	185	187
20	76	73	148	149
35	59	57	119	119

The resultant equilibrium flammability data are summarized in Table IX. The data tabulated show the flammability limits at sea level and their slopes for the four test fuels. These fuels were made up of Jet A and Jet B in the following proportions: 0/100, 50/50, 75/25 and 100/0. It can be observed from Table IX that, as the relative concentration of Jet B is reduced and that of Jet A is increased, the limit temperatures increase and the slopes decrease. The variation of the temperature ranges of the flammability limits at sea level with the relative concentrations of Jet A and B is illustrated in figure 9. It also shows mixing two fuels of divergent vapor pressures does not broaden the temperature range of the resultant envelope. Instead, the temperature range shifts as a non-linear function according to the relative vapor pressure of the mix.

TABLE IX

BLENDING OF JET A AND JET B FUELS

Fuel		Equilibrium Flammability Data			
		Lean Limit		Rich Limit	
Jet A, %	Jet B Batch 2 %	Intercept at Sea Level, °F	Slope, K.ft./°F	Intercept at Sea Level, °F	Slope, K.ft./°F
-	100	-20	-1.22	38	-1.00
50	50	-4	-1.02	51	-0.93
75	25	17	-0.93	83	-0.81
100	-	97	-0.91	172	-0.71

By interpolating the sea level intercepts the flammability envelope of the mix 85% Jet A/15% Jet B was evolved. This envelope is shown in figure 10, in conjunction with the envelopes of the basic fuels. This particular blend is of significant interest since it straddles the nonflammable region that normally separates the envelopes of the Jet A and Jet B. The significance of this normally nonflammable region and its coincidence with the 85/15 mix is made more apparent when evaluated in terms of the probable fuel temperature occurring in-flight. The Coordinating Research Council reported fuel temperature ranges estimated to include 95% of all operations in the altitude range of 35,000 to 40,000 feet (1). In figure 11, these ranges are presented in conjunction with the limits of flammability for the respective fuels at 40,000 feet. This figure illustrates that the 85/15 blend tends to produce equilibrium flammability limits that have a higher probability of being within aircraft operating temperatures than do either of the base fuels.

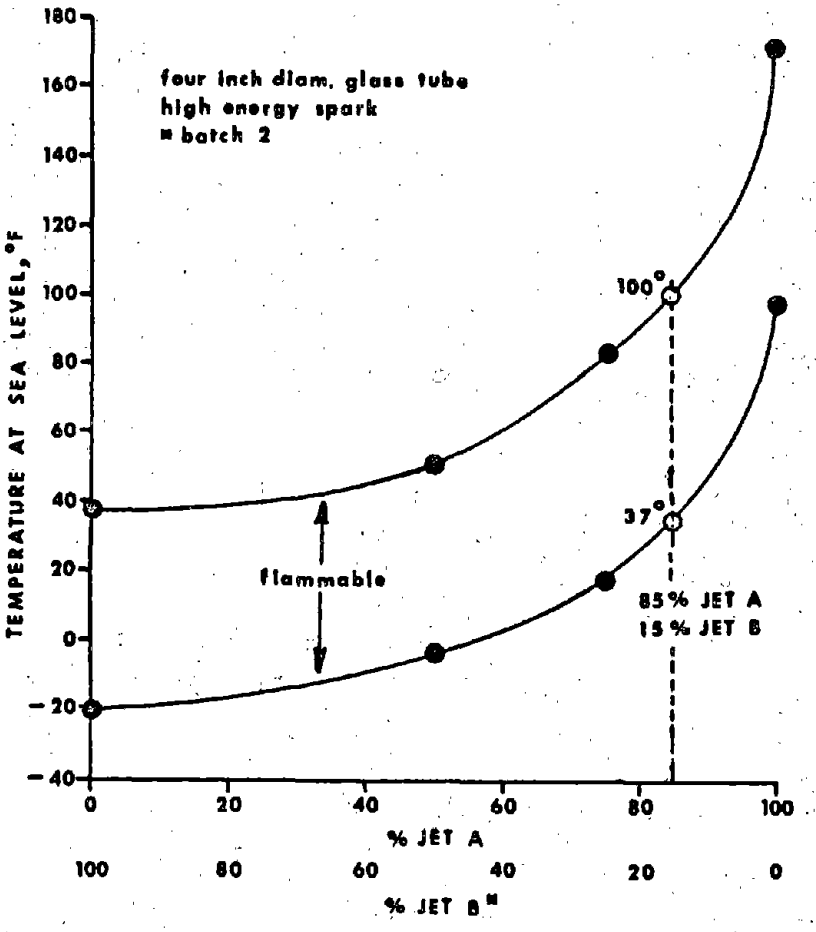

Figure 9 - Variation of the Flammability Limits at Sea Level for Blends of Jet A and Jet B

Effect of Simulated Aircraft Dynamics on Flammability

During routine airline service, practically all flights experience some degree of rough air. Based on a five day observation program by the U.S. Weather Bureau, the probability of aircraft experiencing more than moderate turbulence, is 5% (20). This phase of the investigation was to assess the effect that aircraft flight environments can have in modifying fuel flammability from that observed under equilibrium conditions.

1. Behavior of Liquid Fuel in a Tank - A series of fuel slosh tank experiments were conducted to develop some background into the physical phenomena of sloshing and vibration. A detailed review of the results of these fuel slosh experiments is presented in Appendix VI.

These experiments primarily consisted of recording the conditions within an agitated model fuel tank, by means of high speed photography. Through the resultant photographs it was possible to estimate the proportion of the tank ullage where spray existed. This degree of spray formation was then related to a number of variables: frequency of vibration, rocking, tank baffles, ullage and fuel type. Vibration amplitude, although an important parameter, was not included because of limitations of the facilities.

The important results of this study indicated that there existed two types of spray, designated according to the manner in which it was formed. Spray can be formed by rocking, such as when fuel sloshes back and forth in the tank. Spray can also be produced by vibration. The vibration spray may be visualized as form-

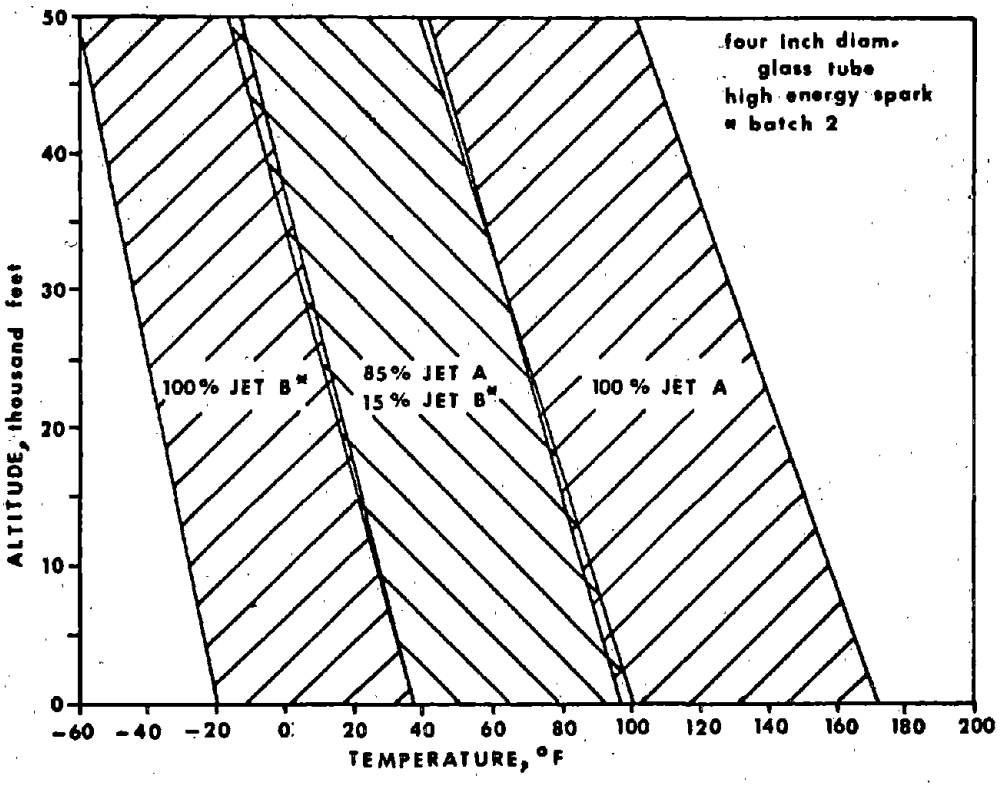

Figure 10 - Flammability Envelope of the Fuel Blend, 85% Jet A/15% Jet B

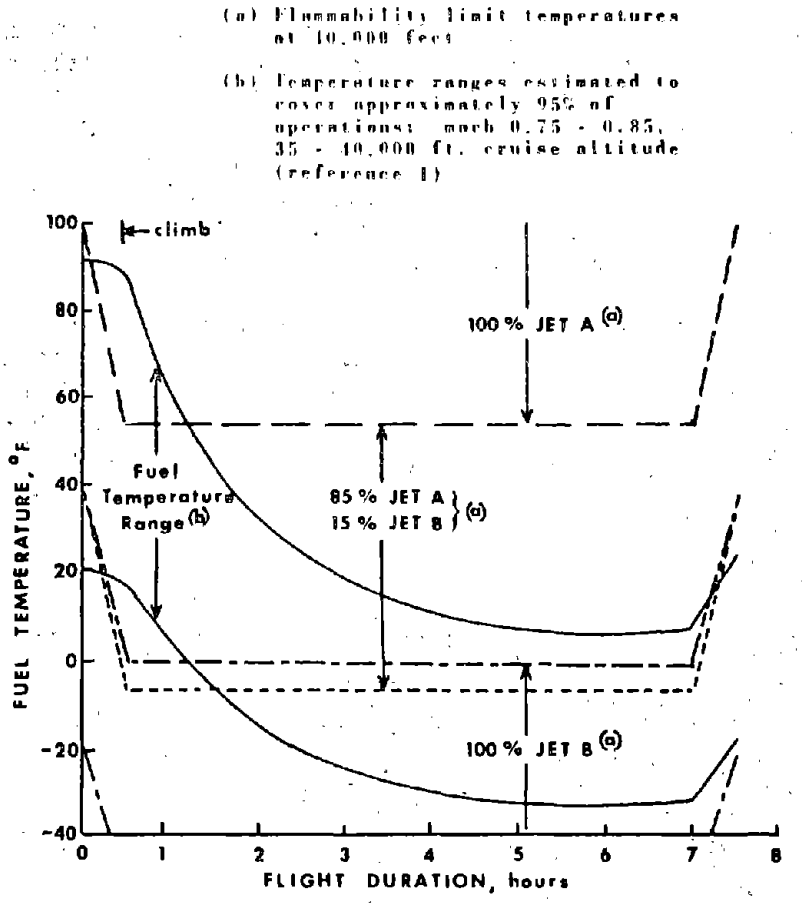

Figure 11 - Estimated In-Flight Fuel Temperatures Compared to the Equilibrium Flammability Envelopes

ing from finger-like projections of liquid, which appear at the surface of the fuel from longitudinally transmitted vibration energies. The fuel projection elongates and then disintegrates, propelling spray droplets up through the vapor space. Vibration, within the range of 12.5 to 15 c.p.s. at ±1/8 inches, produced far more spray than rocking at the rate of 5 to 25 cycles per minute. Oddly enough, within these ranges, increasing the rate of rocking tended to reduce spray. It was observed that increased rocking produces a layer of foam on the surface of the fuel which in turn absorbs the vibrational energy being transmitted to the surface of the fuel. The layer of foam also acts as a barrier to any propelled spray droplets. With respect to fuel type, the wide-cut turbine engine fuel, was more subject to spray formation than the aviation kerosene. This was due to the fact that under the influence of rocking motion, the aviation kerosene produced considerably more foam than the wide-cut turbine engine fuel. The foam in turn reduced the spray produced by vibration.

The magnitude of these simulated aircraft dynamic conditions should not be considered extraordinary. This can be seen by comparing the experimental vibrations to the recorded flight data listed in Table X. Kunkle (24) also reports observations during low altitude turbulent flight, of a commercial aircraft, where wing vibrations could be as much as ±2.7 inches at 3 c.p.s. Therefore, the levels of spray observed during the course of these slosh tank experiments should be considered quite realistic with respect to conditions existing within a tank during turbulent flight.

TABLE X

TYPICAL WING VIBRATION SPECTRUM
APPLICABLE TO MILITARY AIRCRAFT

Aircraft	Frequency c.p.s.	Double Amplitude, inches
F-100 (ref. 21)	0.5 to 14	0.1
F-106 (ref. 22)	0.5 to 10	0.08
B-58 (ref. 23)	0.5 to 0.7	0.3

2. Dynamic Combustion Apparatus - The dynamic combustion apparatus was designed to establish the flammability characteristics of turbine fuels under both equilibrium and dynamic environments. A detailed review of this apparatus and experimental procedure is made in Appendix VII.

On the basis of the conclusions drawn from the model tank studies, vibration was selected as the form of aircraft dynamics most suitable for producing fuel sprays. By mounting the combustion bomb within a temperature control chamber on an electromagnetic shaker, it was possible to conduct ignition studies through a wide spectrum of conditions. Flammability parameters could then be related to fuel spray in addition to fuel type, temperature and altitude.

On the basis of a prior calibration of spray height versus vibration frequency and amplitude, flammability of turbine engine fuels were studied with respect to the following conditions:

a. Static combustion which was characterized by equilibrium vapor space conditions.

b. Dynamic combustion which was characterized by the presence of sprayed fuel within an equilibrium vapor space.

(1) The point of ignition outside the spray envelope.

(2) The point of ignition inside the spray envelope.

3. The Relative Flammability Envelope - The classical definition of flame, requiring the visual confirmation that the flame propagate independently of the ignition source, could not be applied to the dynamic combustion apparatus. With this capability absent, the same equilibrium flammability envelopes developed with the glass tube apparatus could not be determined. However, it was found that the "relative flammability envelope" which was determined on the basis of the instrumental data of pressure and temperature changes, could be substituted for the "equilibrium flammability envelope". Primarily, this relative flammability envelope is based upon the observation that as the fuel/air ratio increases at constant altitude, there is a corresponding transition from a region of low ignition reactions to a region of high ignition reactions. With a further increase in fuel/air ratio the high reaction region again reverts to one of low reactions. This appears to correspond to transitions of the regions of flammability as defined in the discussions of equilibrium flammability envelopes.

The pressure and temperature rises which were produced at ignition were recorded simultaneously on a dual trace oscilloscope. Some examples of these oscillograms which were obtained during the study of Jet A-1 are shown in figure 12. The upper left oscillogram represents ignition at the simulated altitude of 30,000 feet and temperature of 50°F. No instrumental response could be noted at these environmental conditions. However, when the tank temperature was increased to 62°F at the same altitude of 30,000 feet, ignition was accompanied by a temperature increase of 135°F and a pressure increase of 15 p.s.i. This is shown in the upper right oscillogram of figure 12. Similar effects are noted on the bottom two oscillograms of the same figure. These represent ignition at sea level. The bottom left oscillogram represents ignition where the temperature was maintained at 87°F. The temperature and pressure changes which resulted are very slight, being 25°F and 1 p.s.i. The magnitude of these low ordered transients bordered on the sensitivity limitations of the existing instrumentation. When the environmental temperature was increased from the previous 87°F to 95°F, high ignition responses were produced, namely 285°F and 8 p.s.i.

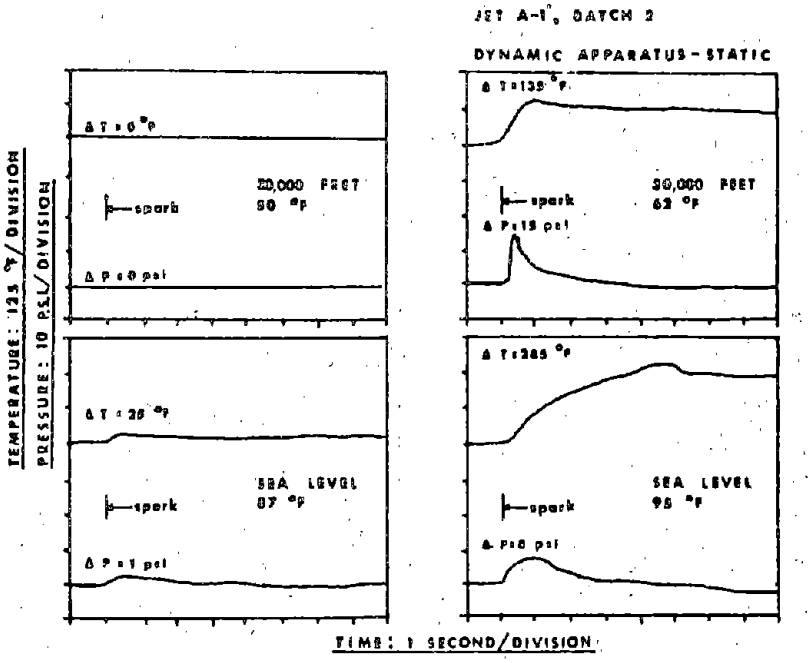

Figure 12 - Representative Oscillograms Showing the Ignition Phenomenon at Equilibrium Conditions

When pressure transients which were produced at a common altitude range were plotted as a function of temperature, the transition between the low and high reaction regions became apparent. This effect can be seen in figure 13 where the pressure transients are recorded which were produced at the two ranges of 20,000 to 30,000 feet and sea level to 10,000 feet. In both cases, there appears to be a definite grouping of pressure transient data according to their relative magnitudes. The low reaction region appears to encompass pressure transients from zero to 4 p.s.i. When temperatures exceeded 62°F in the upper figure and 90°F in the lower figure, the pressure transient values increased almost tenfold from those of the low reaction region. The environmental conditions where the pressure transients exceed this empirical Δ4 p.s.i. appears to define a limiting value between the low and high reaction regions. In a similar fashion, figure 14 shows that the transition temperature of Δ50°F defines a similar limit between the low and high reaction regions. On the basis that an increase of either 4 p.s.i. or 50°F defines the transition between the low and high reaction regions,

the relative flammability envelopes were determined. The limits shown in the relative flammability envelopes are the transition limits.

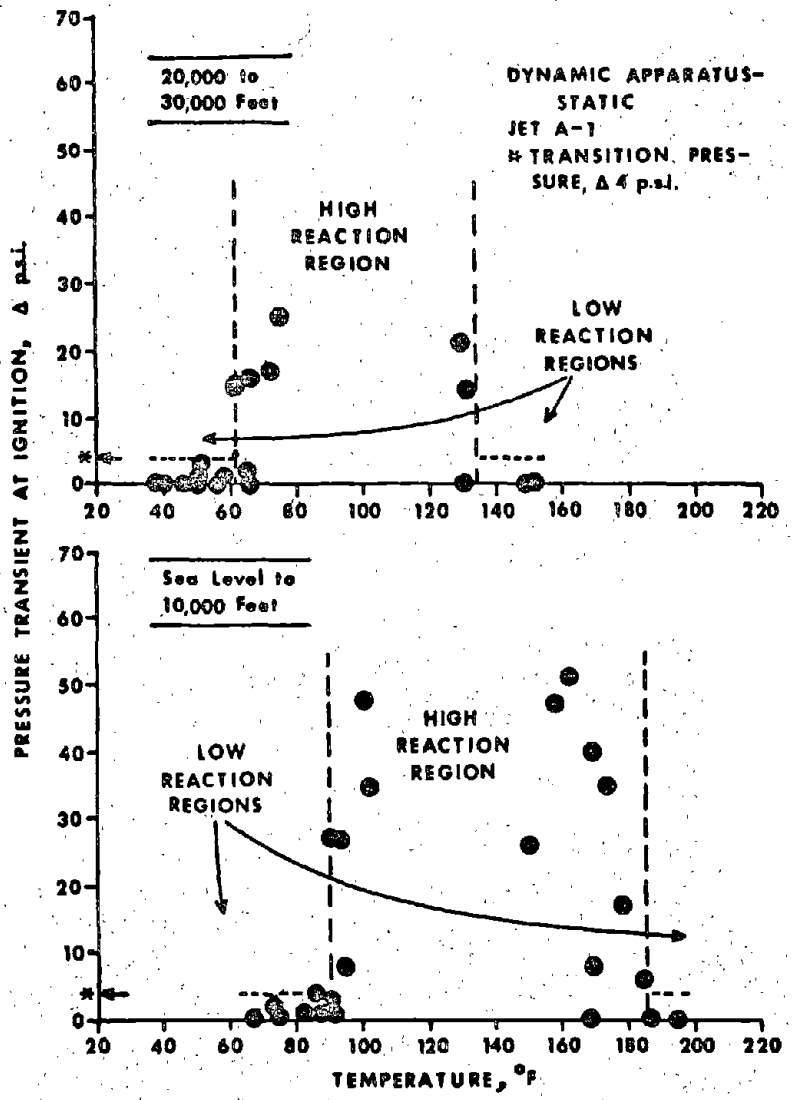

Figure 13 - Shift of Pressure Transients from the Low to the High Reaction Regions

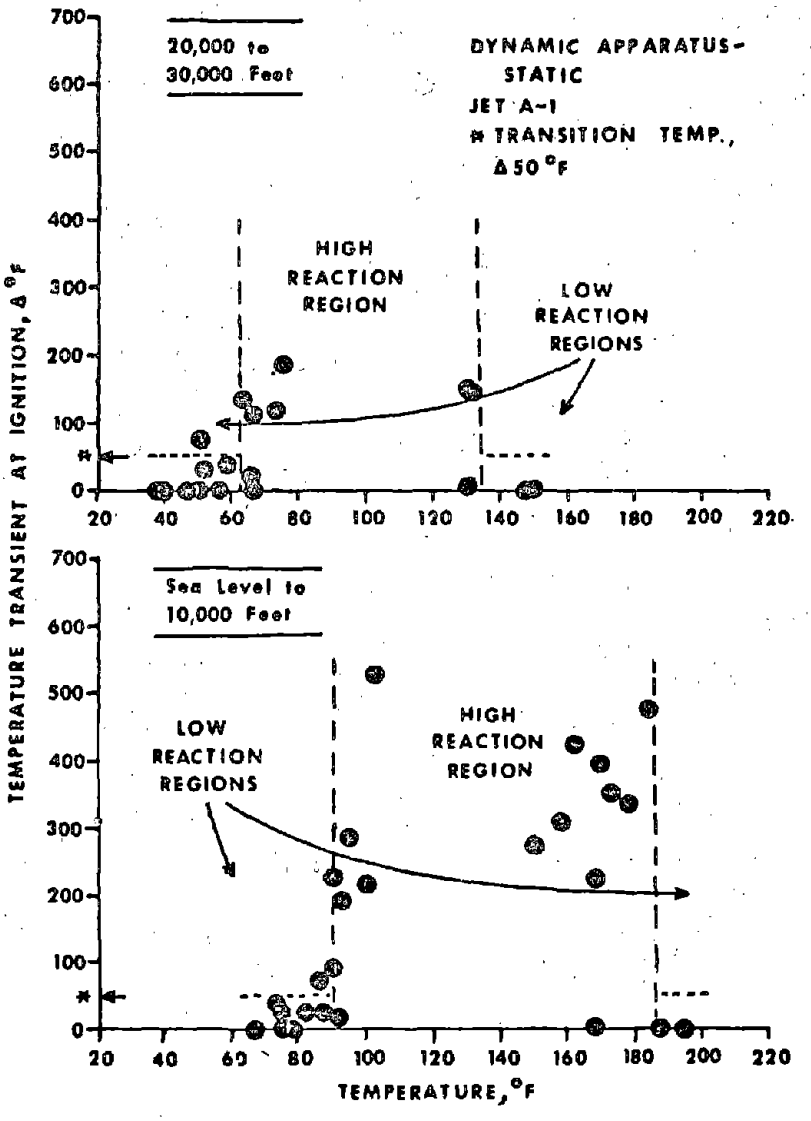

Figure 14 - Shift of Temperature Transients from the Low to the High Reaction Regions

4. Relative Flammability of Jet A-1 at Equilibrium - The relative flammability envelope under equilibrium conditions for Jet A-1, as determined with the dynamic combustion apparatus, is shown in figure 15. In the same figure, the equilibrium flammability envelope, as determined with the glass tube combustion apparatus is also presented for comparison purposes. It can be noted that the two limits are similar, in spite of the fact that the types of apparatus and the combustion definitions are not alike.

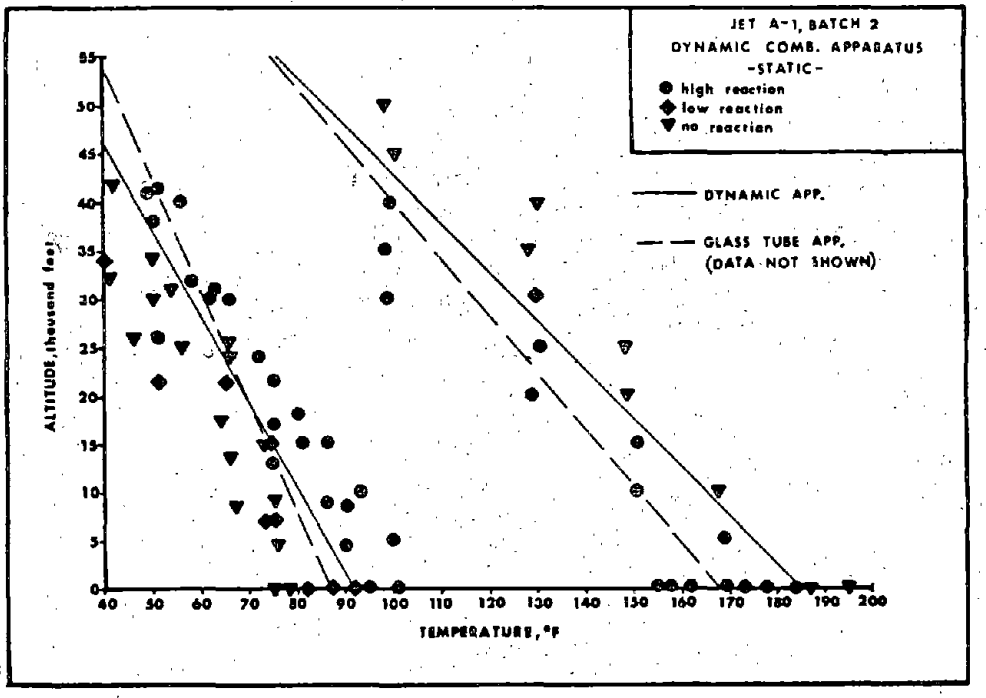

Figure 15 - Relative Flammability Envelope of Jet A-1 at Equilibrium

The pressure and temperature rises were plotted as a function of the temperature differential between the test and limit temperatures corresponding to the simulated altitude of the test. These plots are shown for Jet A-1 in figures 16 and 17, where the data obtained at all altitudes are grouped together. Insufficient data were available to group these data according to specific altitudes. The estimated profile of equilibrium data points shown in figures 16 and 17 provides the basis for comparison with the data obtained under dynamic conditions.

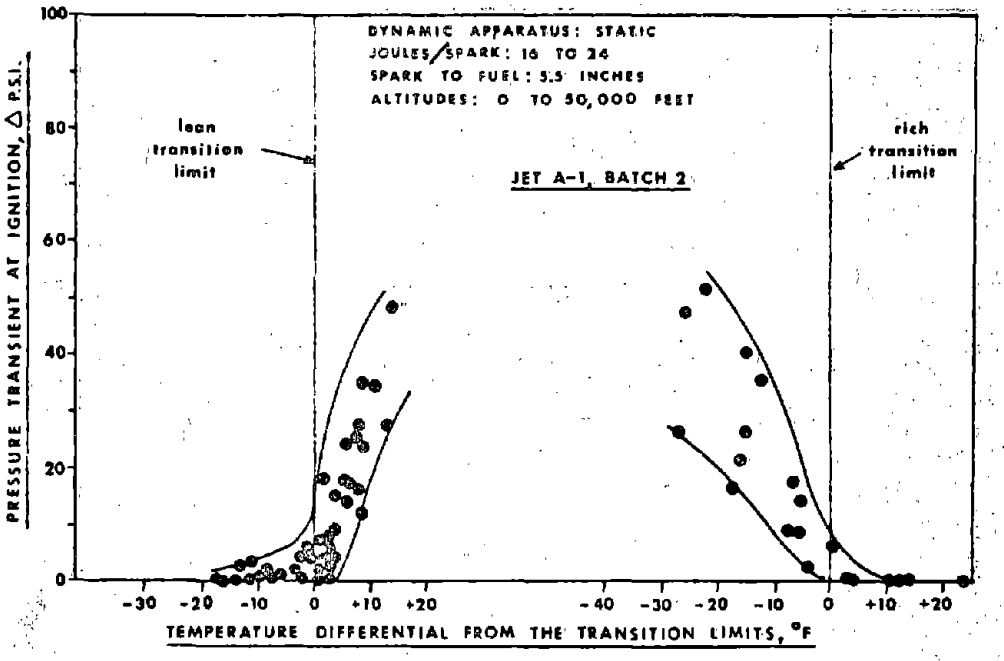

Figure 16 - Pressure Profile of Jet A-1 under Static Conditions

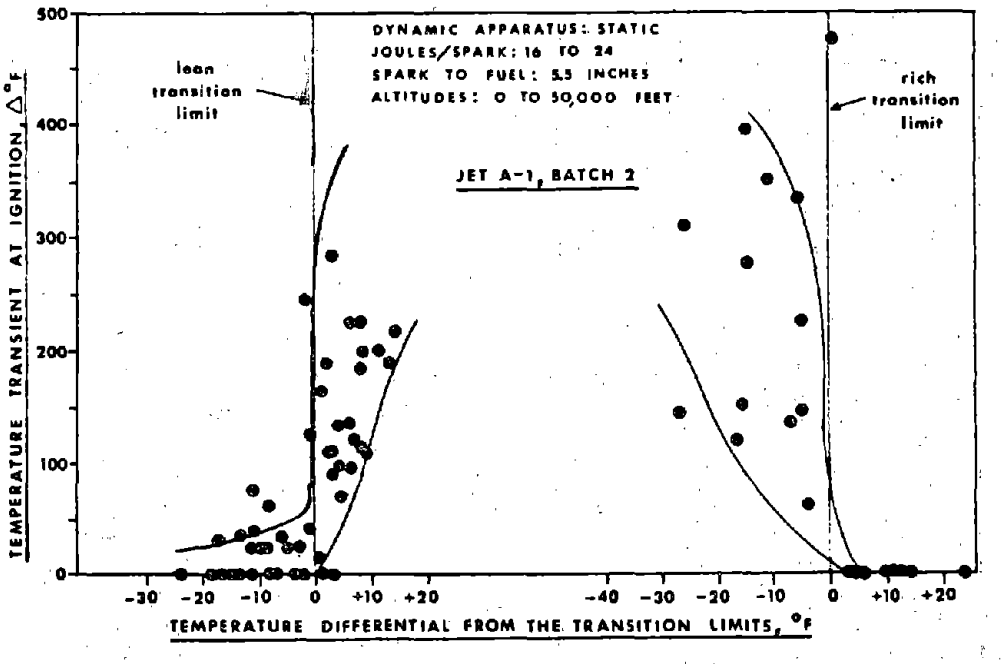

Figure 17 - Temperature Profile of Jet A-1 under Static Conditions

The pressure profile of Jet A-1 demonstrates that as the environmental temperatures are increased, representing a transition through the relative flammability envelope, the resultant pressure rises reach a maximum within the envelope. The magnitude of the pressure rise is a function of the initial pressure. This effect was shown in figure 13, and contributes to the vertical scatter of the data. The temperature profile for the equilibrium combustion of Jet A-1 is similar to that of the pressure profile. The magnitude of the temperature reaction increases with increasing penetration of the relative flammability envelope.

5. Relative Flammability of Jet B at Equilibrium - The relative flammability envelope of Jet B at equilibrium is shown in figure 18. This envelope is also defined by the transition limits based on pressure rises greater than 4 p.s.i. and/or temperature rises greater than 50°F. The pressure and temperature profiles, representing equilibrium ignition conditions, are shown in figures 19 and 20. The primary difference between the Jet B and Jet A-1 envelopes, other than their different locations on the temperature scale, appears in the magnitude of their respective pressure profiles. It appears that, for an equivalent temperature difference within the envelopes, Jet B produced approximately 30% higher pressure transients near the lean limit and 80% greater pressure transients near the rich limit, than were recorded for Jet A-1.

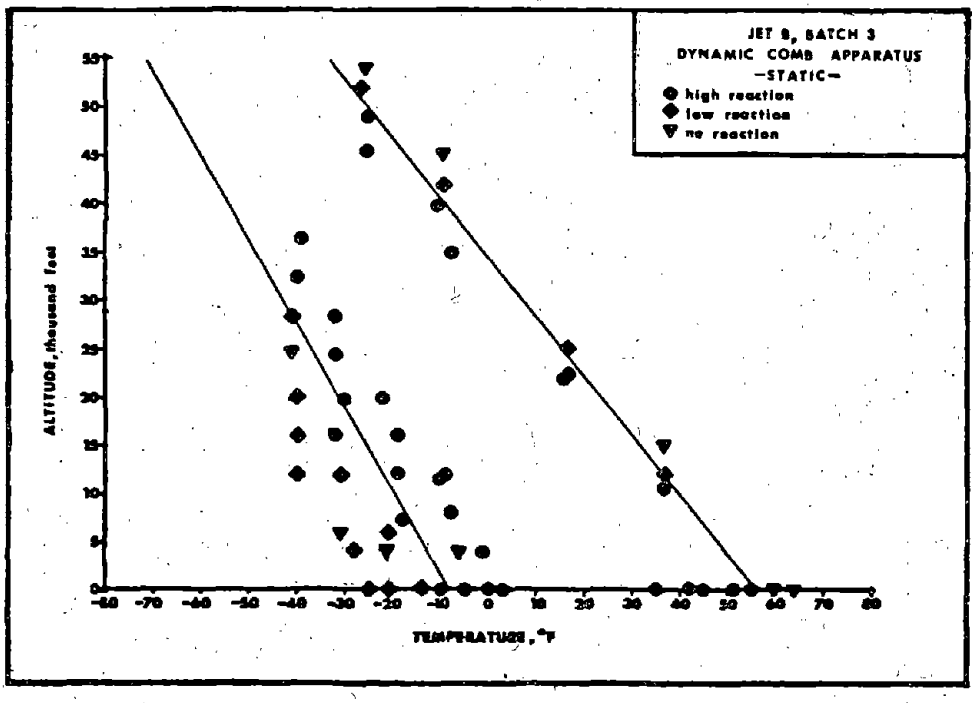

Figure 18 - Relative Flammability Envelope of Jet B at Equilibrium

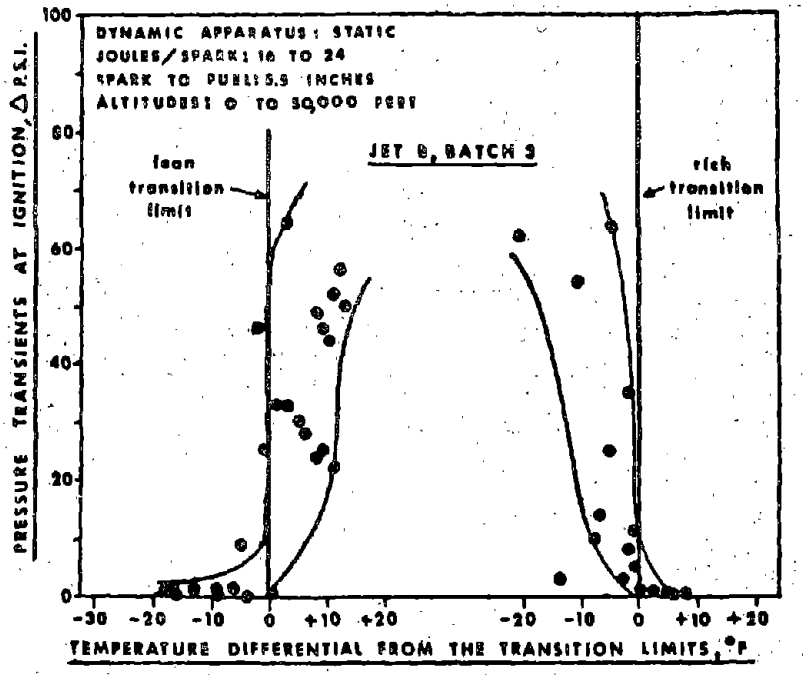

Figure 19 - Pressure Profile of Jet B under Static Conditions

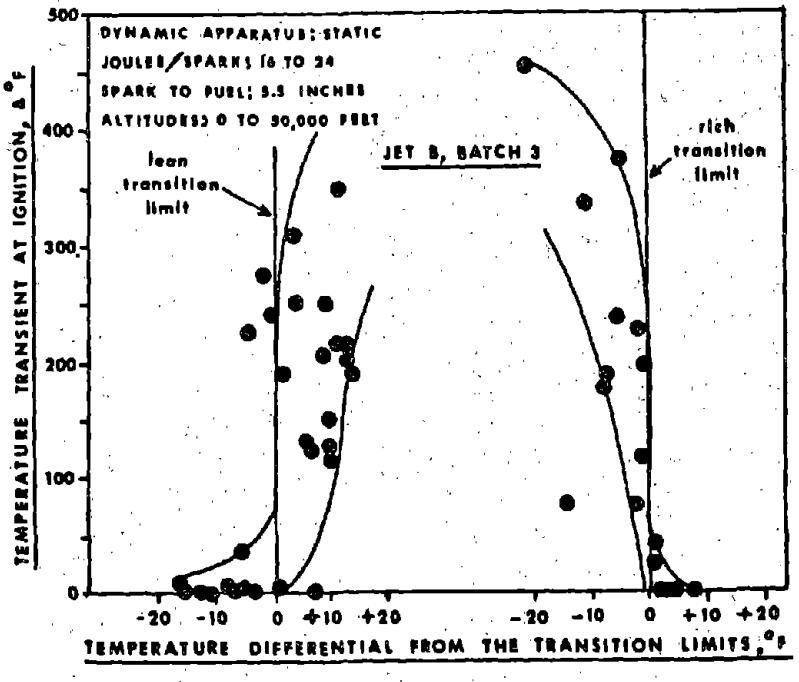

Figure 20 - Temperature Profile of Jet B under Static Conditions

6. Relative Flammability of Jet A-1 under Dynamic Conditions with Ignition Outside the Spray Pattern - By maintaining a vibration frequency of 10 c.p.s. at ±1/16 inch, a spray was produced which did not reach the igniter. With this level of spray, the pressure and temperature transients were determined at the simulated altitudes of sea level and 25,000 feet. These data are shown in figures 21 and 22 in conjunction with the lean region of the static pressure and temperature profiles. It can be seen by the distribution of the data that there is very little difference between the two conditions. Similar effects were noted at the rich region. Therefore it can be concluded that, when the point of ignition is not in the vicinity of sprayed fuel, the pressure and temperature profiles are identical to static conditions, where equilibrium exists.

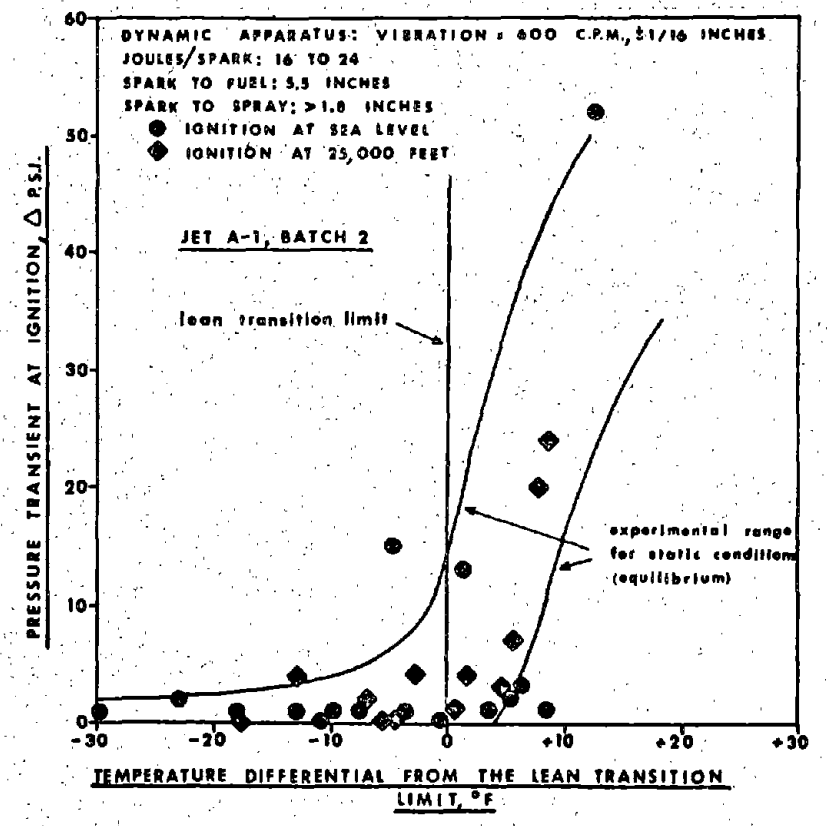

Figure 21 - Dynamic Pressure Profile of Jet A-1: Ignition Outside Spray Pattern

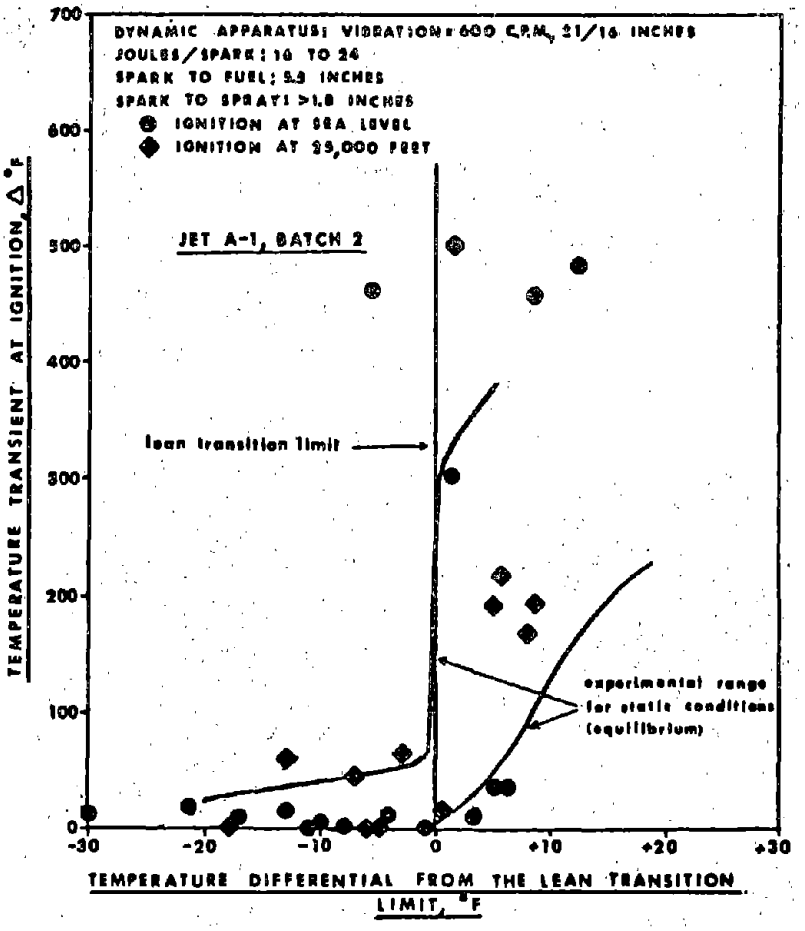

Figure 22 - Dynamic Temperature Profile of Jet A-1: Ignition Outside Spray Pattern

7. Relative Flammability of Jet A-1 under Dynamic Conditions with Ignition Inside the Spray Pattern - The vibration frequency of 15 c.p.s. at ±1/8 inch produced a spray pattern of the fuel which completely enveloped the igniter plug. Pressure and temperature transients were obtained at the simulated altitudes of sea level and 25,000 feet. The data with ignition inside the spray pattern are reported in figures 23 and 24. In the dynamic pressure profile of figure 23, it is quite obvious from the distribution of data with respect to the pressure profile under static conditions, that ignition within the spray pattern has a marked effect. Using the definition that the transition limit is characterized by a minimum pressure rise of 4 p.s.i., the lean transition limit was extended 54°F at sea level and 32°F at 25,000 feet. No equivalent extension occurred at the rich region. From a similar analysis with respect

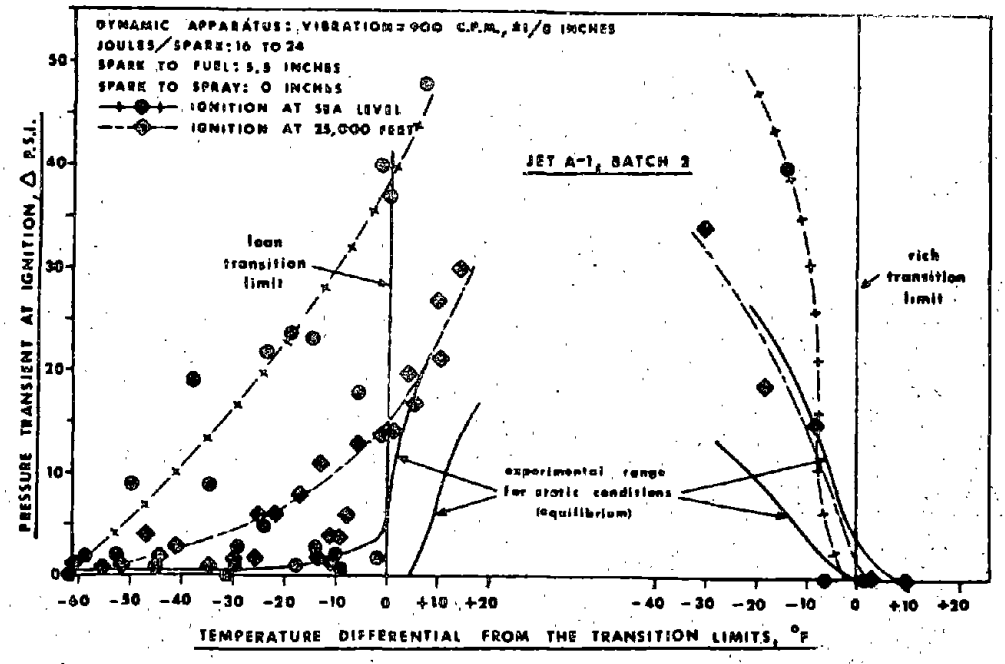

Figure 23 - Dynamic Pressure Profile of Jet A-1: Ignition Inside Spray Pattern

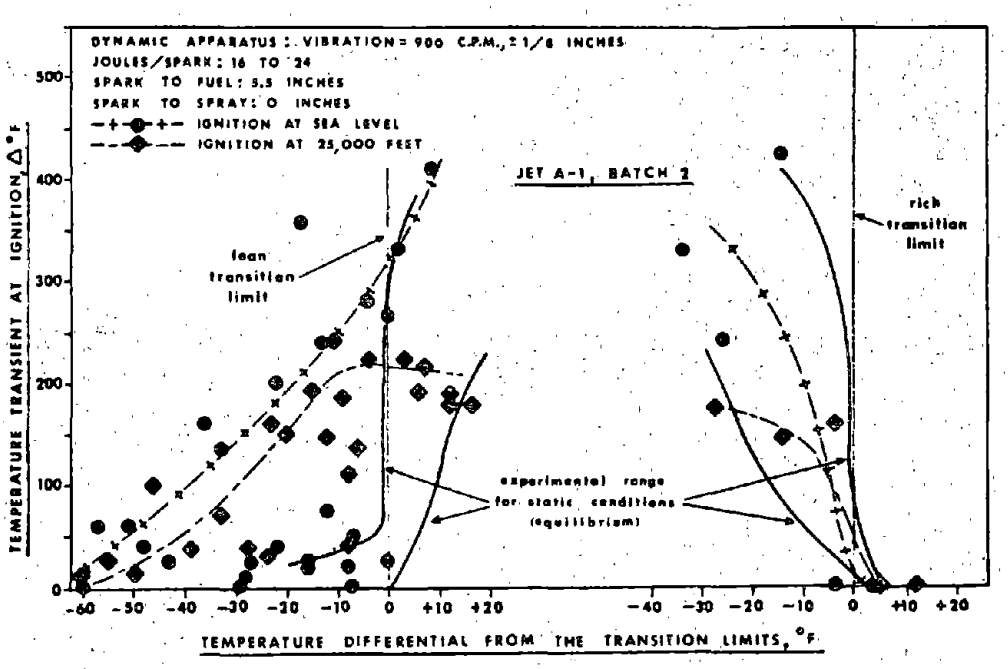

Figure 24 - Dynamic Temperature Profile of Jet A-1: Ignition Inside Spray Pattern

to temperature transients, in figure 24, the lean transition limit was extended 50°F at sea level and 42°F at 25,000 feet. By maximizing the combined effects of pressure and temperature transients, the lean transition limit was extended 54°F at sea level and 42°F at 25,000 feet. No change was noted with respect to the rich transition limit.

8. Comparative Effects of Spray on Turbine Fuel Flammability - A dynamic flammability envelope for a fuel tank, with ignition in the fuel spray, was established by extending a straight line through the dynamic limits established at sea level and 25,000 feet. Figure 25 shows this envelope superimposed on the envelopes of Jet A-1 and Jet B. An extension of the lean limit for Jet B is also indicated although the exact new limit was not established. The net effect of ignition in the midst of spray was to extend the lean transition limit of the Jet A-1 into the envelope of Jet B. When the point of ignition was outside the spray pattern, the relative flammability envelope was identical to the envelope representing the static conditions of equilibrium.

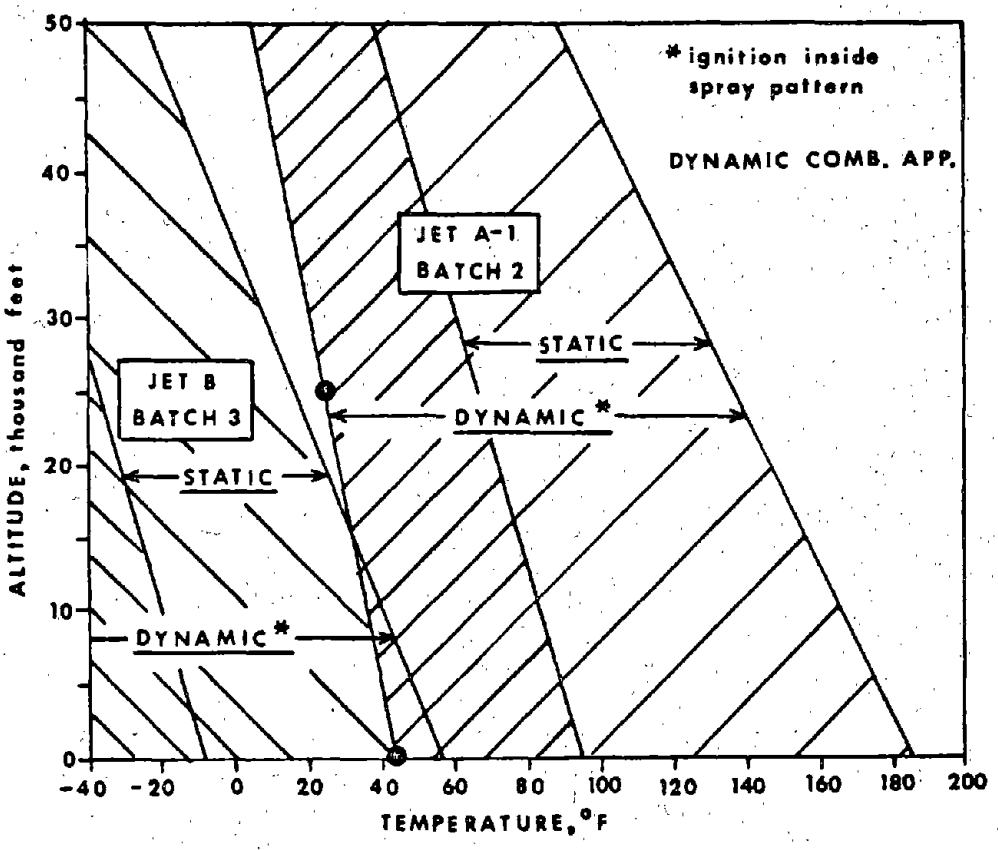

Figure 25 - Effect of Dynamics on the Relative Flammability Envelopes of Jet A-1 and Jet B

As discussed in the section dealing with mixed fuels, the Coordinating Research Council reported fuel temperature ranges estimated to cover 95% of all operations at the cruising altitudes of 35,000 to 40,000 feet (1). In figure 26 the in-flight fuel temperatures are shown in conjunction with the static and dynamic transition limits of the respective fuel at the altitude of 40,000 feet. It can be seen that spray, if a source of ignition were to occur within the spray pattern, severely increases the duration of potentially flammable conditions with respect to the fuel, Jet A-1. However, because of the in-flight temperatures involved, a comparable increase in the incidence of potential flammability due to spray was not noted with the fuel, Jet B.

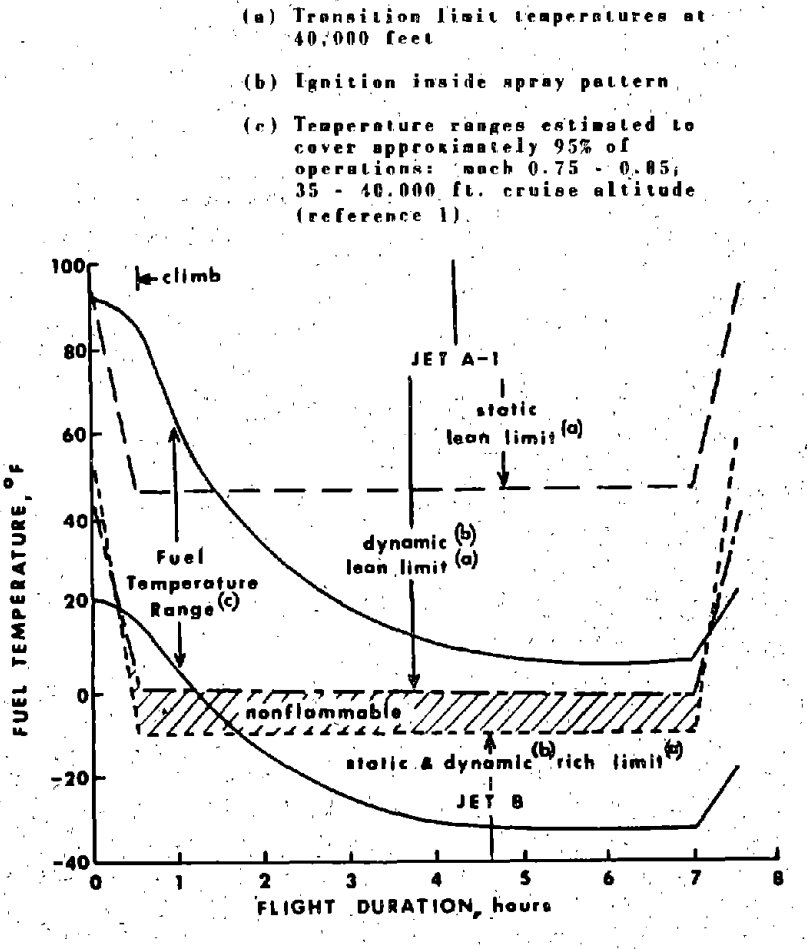

Figure 26 - Estimated In-Flight Fuel Temperatures Compared to the Static and Dynamic, Relative Flammability Envelopes

Effect of Aircraft Ascent on the Relative Flammability Envelopes of Jet A-1

During climb, aircraft tank pressures are reduced. The climb is accompanied by a continuous venting out from the tank. This venting maintains a relatively small pressure differential from the continuously decreasing, atmospheric pressure. Reducing tank pressure results in production of condensation-type mists. This misting is also discussed in Appendix VIII. From photographic evidence, these mists are a condensation of the vaporized fuel in the tank ullage. The formation of the mist does not contribute to a change in the existing fuel/air ratios, but only alters the physical nature of the fuel already present in the vapor space. Part of the vapor takes the form of an aerosol. Since small, suspended droplets have flammability characteristics that are identical to those of the vapor, the change in the physical state of the vapor space fuel is not accompanied by changes in its flammability characteristics. If there were no liquid fuel present, the fuel/air ratio would remain the same as originally existed at ground level. As fuel vapors and air are removed with liquid present, the fuel tends to release more vapors to compensate for those lost to maintain the vapor pressure of the fuel. This results in a gradual increase in fuel/air ratio as the vapors diffuse from the liquid surface through the vapor space. The time required for this newly vaporized fuel to diffuse through the vapor space to the position where ignition occurs, is the rate controlling factor in altering the resultant flammability envelope. Other factors which can change the effective fuel/air ratio are oxygen enrichment due to outgassing of oxygen-rich air from the fuel; and fuel foam and spray from sudden outgassing. The latter did not occur in the quiescent simulated climb of this test.

To investigate some of these effects, the relative flammability envelope of Jet A-1 was determined under simulated climb conditions. The analog was an aircraft taking off from ground level and climbing at the rate of 3,000 to 4,000 feet per minute. These results are shown in figure 27. Here there was produced a general shifting of the limits. Since it is more consistent to discuss the shift in terms of altitude, the lean transition limit was displaced by 10,000 feet from the static, equilibrium transition limit. The rich limit was displaced by 3,500 feet. Apparently, at the climb rate of 3,000 to 4,000 feet per minute, the shift in the limits is caused by a time lag. This is the time required for additional fuel enrichment to produce the limiting fuel/air ratio at the location where the ignition will occur. In the case of these experiments, the point of ignition was 5.5 inches above the level of the fuel. Thus, for the lean limit, diffusion of additional fuel to produce the lean limit fuel/air ratio required 2.5 to 3 minutes. For the rich limit fuel/air ratio only 1 minute was required.

We can conclude that, during climb, there is an upward shift of the relative flammability envelope. This shift is due primarily to the time required to enrich the vapor space by additional vaporized fuel. The mists that are produced by the constantly reducing tank pressures do not have any effect on tank flammability.

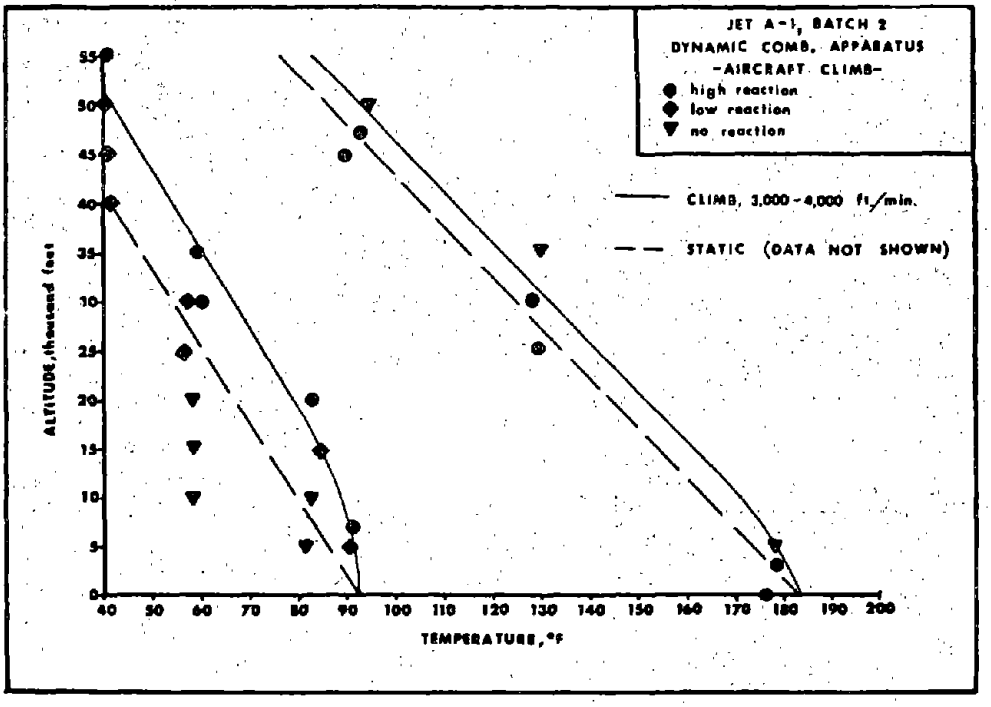

Figure 27 - The Relative Flammability Envelope of Jet A-1 During Aircraft Climb

CONCLUSIONS

1. Dynamic conditions in a fuel tank can produce sprays which cause a significant expansion (at least 50%) of the temperature range at which the tank vapor space is in a flammable condition. This expansion occurs at the lean limit of the flammability envelope. For practical purposes it makes the equilibrium flammability envelope of the fuel invalid for turbulent flight conditions or any conditions which result in fuel droplets in the tank.

2. During aircraft climb a non-equilibrium condition can exist, such that a flammability limit is reached at a higher altitude than would be predicted on an equilibrium basis. During aircraft climb the concentration of fuel vapors in a tank can be lower than that which would exist under equilibrium conditions. This causes a minor temporary shift in the flammability limits.

3. Reported equilibrium flammability limits of turbine fuels are further affected by:

a. Variations in experimental equipment and technique.

b. Variations in properties of specific fuel samples within a type.

c. History of the fuel. Properties may change because of prior flight.

d. Blending of fuel types. Small quantities of Jet B in a tank of Jet A can create a flammable mixture in a temperature range where neither fuel is flammable.

REFERENCES

1. "Aviation Fuel Safety", CRC Project No. CA-37-64, Coordinating Research Council, New York, June 1964.

2. Coordinating Research Council, "Solution and Evolution of Gases and Vapors in Aircraft Fuels", WADC-TR-193, Wright-Patterson Air Force Base, Ohio, April 1959.

3. Green, H.L., Lane, W.R., "Particulate Clouds: Dusts, Smokes and Mists", p. 4, Van Nostrand, Princeton, 1964.

4. Maggitti, L., Nestor, L.J., AEL Intralab. Report, Aeronautical Engine Department, Philadelphia, 27 July 1965.

5. Coward, H.F., Jones, G.W., "Limits of Flammability of Gases, and Vapors", Bulletin 503, Bureau of Mines, U.S.G.P.O., Washington, 1952.

6. Zabetakis, M.G., "Flammability Characteristics of Combustible Gases and Vapors", Bulletin 627, Bureau of Mines, U.S.G.P.O., Washington, 1965.

7. Zabetakis, M.G., Jones, G.W., Scott, G.S., Furno, A.L., "Research on the Flammability Characteristics of Aircraft Fuels", WADC TR-52-35, Wright-Patterson Air Force Base, Ohio, January 1956.

8. Gerstein, M., Levine, O., Wong, E.L., "Fundamental Flame Velocities of Pure Hydrocarbons: I, Alkanes, Alkenes, Alkynes, Benzene and Cyclohexane", NACA RM E50G24, Lewis Flight Propulsion Laboratory, Cleveland, September 1950.

9. Levine, O., Gerstein, M., "Fundamental Flame Velocities of Pure Hydrocarbons: III, Extension of the Tube Method to High Flame Velocities, Acetylene-Air Mixtures", NACA RM E51J05, Lewis Flight Propulsion Laboratory, Cleveland, December 1951.

10. Brockman, W.E., Duval, D.S., "Physical and Chemical Properties of JP-4 Jet Fuel for 1963", AFAPL-TR-64-148, Wright-Patterson Air Force Base, Ohio, January 1961.

11. Brockman, W.E., Duval, D.S., "Physical and Chemical Properties of JP-4 Jet Fuel for 1964", AFAPL-TR-65-106, Wright-Patterson Air Force Base, Ohio, September 1964.

12. Brockman, W.E., Duval, D.S., "Physical and Chemical Properties of JP-4 Jet Fuel for 1965", AFAPL-TR-66-83, Wright-Patterson Air Force Base, Ohio, September 1965.

13. ---, "Spark Energy Measurement Using Oscilloscopic Methods", Aerospace Information Report 77, Society of Automotive Engineers, New York, December 1961.

14. Barnett, H.C., Hibbard, R.R., "Properties of Aircraft Fuels", NACA-TN3276, Lewis Flight Propulsion Center, Ohio, August 1956.

15. ---, "1967 Book of ASTM Standards: Part 17", American Society for Testing and Materials, Phila.

16. Hottel, H.C., Williams, G.C., Simpson, H.C., "Combustion of Droplets of Heavy Liquid Fuels", Fifth International Combustion Symposium, pp. 101-129, Rheinhold, New York, 1955.

17. Affens, W.A., "Flammability Properties of Hydrocarbon Fuel: Part I", NRL-6270, U.S. Naval Research Laboratory, Washington, D.C., May 1965.

18. Zengel, A.E., Lander, H.R., Scribner, W.G., Warren, J.H., "An Examination of Methods for Calculating Vapor Pressure of Petroleum Hydrocarbons", APL-TR-64-37, Wright-Patterson Air Force Base, Ohio, March 1964.

19. Glasstone, S., "The Elements of Physical Chemistry", Van Nostrand, p. 136, New York, 1950.

20. Kraght, P.E., "Requirements for Significant Turbulence", Shell Aviation News, 334, pp. 16-20, 1966.

21. Thomas, C.F., "Flight Vibration Survey of F-100-C-1 Aircraft", ASD TN-61-61, Wright-Patterson Air Force Base, Ohio, May 1961.

22. Reich, H.K., "Flight Vibration Survey of F-106A Aircraft", ASD TDR-62-504, Wright-Patterson Air Force Base, Ohio, April 1962.

23. Reich, H.K., "Flight Vibration Survey of B-58 Aircraft", ASD TDR-62-384, Wright-Patterson Air Force Base, Ohio, April 1962.

24. Kunkle, R.D., personal communication, The Boeing Company, Renton, September 1967.

25. Blackington, P.A., "Oscillographic Method for Measuring Spark Energy of Capacitor Discharge Ignition Systems", Report No. 8-9274, Scintilla Division, Bendix Aviation Corp., Sidney, New York, 1960.

26. Klose, W., Meldor, F.S., "Inflammability of Fuel Vapor and Mixtures of Fuel Vapors and Fuel Mists", Document No. D-11872, Boeing Aircraft Company, Seattle, 29 May 1951.

27. Carhart, H.W., personal communication, U.S. Naval Research Laboratory, Washington, 29 September 1965.

28. ---, "Handbook of Chemistry and Physics", Chemical Rubber Publishing Company, 43rd Edition, 1961-1962.

APPENDIX I

TABLE XI - FUEL ANALYSIS

Fuel Designation	Wide-Cut Turbine Fuels				Aviation Kerosenes				Mixed Fuels	
	JP-4	Jet B			JP-5	Jet A	Jet A-1		50% Jet A 50% Jet B **	75% Jet A 25% Jet B **
Batch	-	Batch 1	Batch 2	Batch 3	-	-	Batch 1	Batch 2		
Gravity, Specific, 60/60°F	0.7620	0.7599	0.7595	0.7612	0.8294	0.8104	0.8058	0.7994		
Gravity, °API, 60/60°F	54.2	54.7	54.8	54.4	39.1	43.1	44.1	45.5		
Reid Vapor Pressure, lb/in²	2.34	2.14	2.28	2.09	-	-	-	-		
Distillation, I.B.P. °F	162	150	150	156	320	322	308	314	166	186
5% over °F	188	180	182	194	368	342	340	336	206	248
10% °F	200	190	192	208	382	350	350	346	218	272
20% °F	214	206	208	226	394	367	364	358	244	310
30% °F	226	220	220	242	406	374	376	368	270	342
40% °F	240	236	232	258	414	384	388	378	302	366
50% °F	256	254	254	276	424	398	400	390	334	380
60% °F	276	272	274	298	432	408	412	400	360	394
70% °F	296	296	298	326	494	422	426	412	380	410
80% °F	326	328	324	366	458	438	442	428	404	426
90% °F	356	360	362	426	476	460	462	450	432	452
95% °F	384	386	386	458	492	476	476	470	456	476
End Point °F	408	418	413	490	516	503	489	492	490	500
Recovery % vol.	99.0	99.0	99.0	99.0	98.6	98.7	98.7	99.0	98.7	98.6
Residue % vol.	1.0	1.0	1.0	1.0	1.4	1.3	1.3	1.0	1.3	1.4
Loss % vol.	0.0	0.0	0.0	0.0	0.0	0.0	0.0	0.0	0.0	0.0
Gum, Existent, mg/100 ml	0.4	0.6	0.2	0.2	2.0	0.8	0.4	0.4		
Potential, mg/100 ml	0.4	0.6	0.8	2.5	2.0	0.8	0.4	2.1		
Sulfur, % Wt.	0.15	0.03	0.01	0.07	0.32	0.07	0.06	0.09		
F.I.A. Saturates, % vol.	81.64	80.75	82.43	87.94	77.20	83.46	82.61	87.21		
Olefins, % vol.	0.89	1.24	1.35	1.42	2.21	1.50	4.35	5.81		
Aromatics, % vol.	17.47	18.01	16.22	10.64	20.59	15.04	13.04	6.98		
Aniline Point, °C	47.4	49.3	49.9	60.0	59.4	62.4	62.9	65.4		
Aniline - Gravity Constant	6,358	6,602	6,675	7,616	5,431	6,219	6,403	6,811		
Heat of Combustion, BTU/lb	18,571	18,674	18,674	18,779	18,456	18,589	18,611	18,632		
Corrosion, Copper Strip	1-B	1-A	1-A	1-B	1-A	1-A	1-A	1-B		
Smoke Point, °F	27.0	27.0	28.0	29.0	20.0	22.0	24.0	26.0		
S.V.I. Calculation	68.02	67.63	68.77	64.98	29.97	49.90	45.00	41.20		
Freeze Point, °F	<-76	<-76	<-76	<-76	-60	-70	-65	-65		
Flash Point, °F	-	-	<-30*	<-30*	135	125	120	118		
Water Tolerance	0.0(#1)	0.0(#1)	0.5(#1)	0.0(#1)	0.5(#3)	0.0(#1)	0.5(#1)	-		
Viscosity, cs., 100°F	0.68	0.70	-	-	1.68	1.40	1.36	1.32		
-30°F	1.83	1.84	-	-	11.80	7.81	7.36	6.79		
Contamination, mg/liter	0.4	1.4	3.5	2.0	0.5	0.6	4.4	1.7		

* Adaptation of Pensky-Martin Closed Cup Method

** Batch 2

APPENDIX II

Glass Tube Combustion Apparatus

General - For the visual definition of flammability envelopes, the glass tube apparatus which is shown in figure 28 was used. The principle of visually defining flames is widely accepted and has been used quite extensively for determining limits of flammability. A flammable point is defined as one where the flame propagation is essentially independent of the ignition source. Independent flame propagation is ascertained when the flame travels a minimum distance of four feet (5, 6). A nonflame is one where no visual confirmation of a flame can be made, or the flame fails to propagate the minimum required distance of four feet. To make the standard glass tube apparatus applicable to fuels, which are composed of wide boiling hydrocarbon fractions, the fuel sample was designed to be retained in the combustion apparatus even during combustion. This made possible the natural formation of equilibrium fuel/air ratios from the liquid fuels and eliminated the need for calculating flammability envelopes from the premixed fuel/air ratios. The calculation of envelopes is of questionable value when applied to the complex system of fuels.

The combustion apparatus was made up of a combustion chamber and a fuel section which were contained in an environmental chamber for temperature control. The combustion chamber was a four-foot length of flanged, Pyrex pipe. In order to minimize "wall effects" which tend to distort the flammability envelopes, the diameter of the glass pipe was standardized at four inches. The fuel section was a one-foot length of flanged Pyrex pipe which mated to the combustion chamber. The base of the fuel section held five air diffusers through which air was bubbled. The fuel section was filled or drained through the valve at the base of the apparatus. On top of the combustion chamber, an extension of aluminum pipe was made to permit the external installation of a pressure relief plate and piping to the vacuum pump and manometer for pressure regulation. The pressure relief plate was an aluminum plate which was machined to seat on the combustor chamber extension with an "O" ring seal. Since the pressures covered in this investigation were invariably negative, proper seating of the plate provided leakproof conditions. Because it was free to move during combustion it immediately responded to relieve any increase in pressure. A detailed view of the electrode housing is shown in figure 29. First, two access holes, diametrically opposed, were blown through the glass pipe. This permitted the use of adjustable electrodes which were affixed to the pipe in such a manner that they be completely insulated from one another. This was done by constructing electrode plates having the outer diameter of the pipe and cementing these to the pipe with

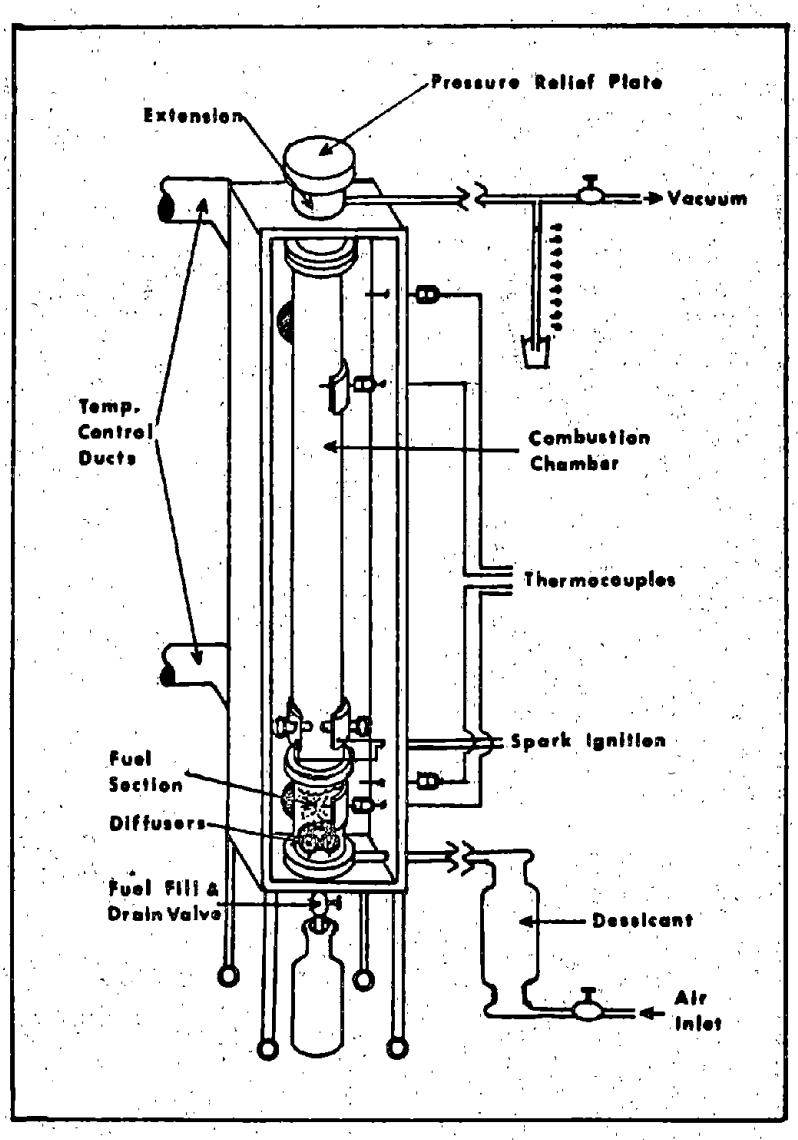

Figure 28 - Glass Tube Combustion Apparatus

silicone rubber cement. Each electrode plate was fitted with a leak-proof stuffing box holding the electrode. This permitted gap adjustment. To maintain high energy sparks, the electrodes were removed and the internal surface of the glass pipe cleaned daily, which prevented the buildup of any residual coating on the internal glass surface. Such a coating could cause a reduction in spark energies by shorting out the electrodes. For monitoring temperatures, thermocouples were mounted in the combustion chamber and fuel section in a manner similar to that described for the electrodes. The environmental chamber was also instrumented with an upper and lower thermocouple readout. Temperature conditions were maintained so that a temperature gradient across the two environmental chamber thermocouples never exceeded 3°F. Temperature control of the environmental chamber was maintained with a Missimer Portable Temperature Servo Conditioner. By utilizing the Servo Conditioner's electrical heating elements or liquid CO_2, environmental temperatures were capable of being maintained within the range of +400°F to -100°F. However, for low temperatures, the excessive consumption of liquid CO_2 introduced a practical temperature limit of approximately -40°F to -50°F.

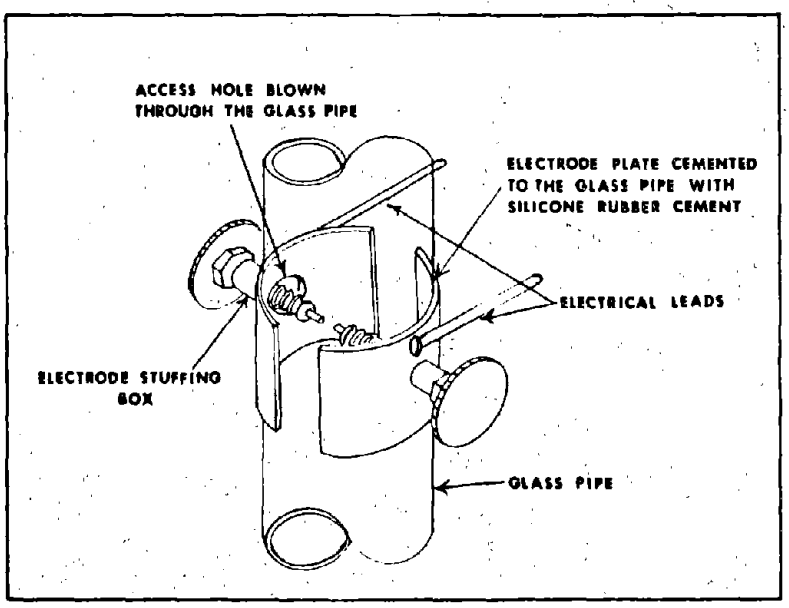

Figure 29 - Detailed View of Electrode Housing

Experimental Procedures - The combustor was first purged of all combustible material. The air was then evacuated with the vacuum pump to a vacuum of 29 to 29.5 inches of mercury at which time the vacuum pump and all associated valves were shut off. With the negative pressure in the combustor, fuel of a predetermined volume was drawn up through the fuel-fill-and-drain valve. The temperature of the fuel sample, prior to introduction, was equal to or cooler than the apparatus temperature. The normal volume of fuel was maintained to produce a vapor space to fuel volume ratio of 7:1, which gives a system ullage of 87.5%. Since the vaporization of a liquid is proportional to its partial pressure, the fuel vapor in the vapor space at this time is greater than required for the test condition. Upon equilibration of the fuel and apparatus temperatures, dry air was introduced through the combustion chamber air inlet to produce the predetermined experimental pressure. The air was injected at the test temperature through fine diffuser stones below the liquid level thereby saturating it with fuel. The addition of air also provides a mixing effect in the combustion chamber. Visual observations utilizing the Tyndall effect were made of the combustion chamber to insure the absence of mists after achieving pressure adjustments. If the rate of air inlet was too rapid, mists would be produced by mechanical carryover. Also during initial evacuation, if fuel remained following the purging process, "altitude-climb" mists were produced, indicating that additional purging was necessary. With the pressure and temperature established in the apparatus, the system was ready for test. The room was darkened and the chamber ignited by an a.c. electric spark of about 1/2 second duration. The characteristic combustion reaction at time of ignition was recorded. Its classification was either flammable or nonflammable. To be nonflammable no evidence of flame was observed, or a flame would be extinguished before propagating the entire four feet. A condition was classified as flammable only if the flame traversed the complete four-foot length of the combustion chamber.

Depending upon whether the equilibrium fuel/air ratio was predominantly lean or rich at the equivalent altitude, the characteristic color of the flames varied. Generally, the laboratory observations made on flame color can be summarized as follows:

Altitude K. ft	Color of Flame	
	Lean Limit Region	Rich Limit Region
0 - 20	Blue	Yellow
20 - 40	Blue-Green	Yellow-Green
40 - 60	Green	Green

APPENDIX III

Measuring the Spark Energy of the A.C. Ignition System

The SAE (13) and Blackington (25) describe oscillographic techniques for measuring the spark energies of capacitor discharge systems. The principles which they describe were applied to the a.c. ignition system used in the glass tube flammability studies. The capacitor discharge type is not a single electrical discharge. Instead, it is composed of series of electrical oscillations. The electrical oscillations are a function of the system's inductance and capacitance. An analogous series of oscillations occur with the a.c. system but is a function of the 60 cycle input. The determination of spark energies of the capacitor discharge system requires the observation of the time variation of both the arc stream current and voltage to obtain a power vs time relationship. The integral of such a relationship on a per spark basis is the energy. The same technique was applied to the a.c. ignition system. Voltages were measured across the spark gap using a high voltage probe of 1 megohm resistance in parallel with the electrodes, with a dual trace oscilloscope readout. Current was determined by measuring the voltage drop across a 1 ohm resistance placed in series in the electrode circuit. Oscillograms of both the current and the voltage were made simultaneously. Typical oscillograms used for the calibration of the energy of the a.c. ignition system are shown in figure 30. In this figure it can be seen that throughout the phase cycle (0 to 4 seconds), discontinuities occur, which are due to sparking. These occur for both the voltage and current. The energy dissipated may be calculated by using these voltage-time and current-time relationships. It is first necessary to make a power curve which is the curve of the instantaneous product of current and voltage versus time. This product curve then represents the variation of power with time and the integral of this curve, i.e. the area beneath the curve, represents the energy dissipated in the spark. The energies for the particular sparks shown in figure 30 were calculated to be as follows:

Spark No.	Energy: Joules/Spark
(1)	9.4
(2)	5.7
(3)	6.0
(4)	5.6
(5)	5.8
(6)	6.2
(7)	9.8

This type of determination was carried out for a series of five phase changes recording the maximum spark energy in each particular phase. In the previous example, only the maximum energy value of 9.8 joules/spark would have been recorded for that phase. On the basis of the five determinations, the average maximum spark energies were established and reported as being the spark energy. Two different transformers were selected to represent "high" and "low" ignition energies, i.e. 20 and 5 joules per spark. The spark gap used at both energy levels was 0.4 inches.

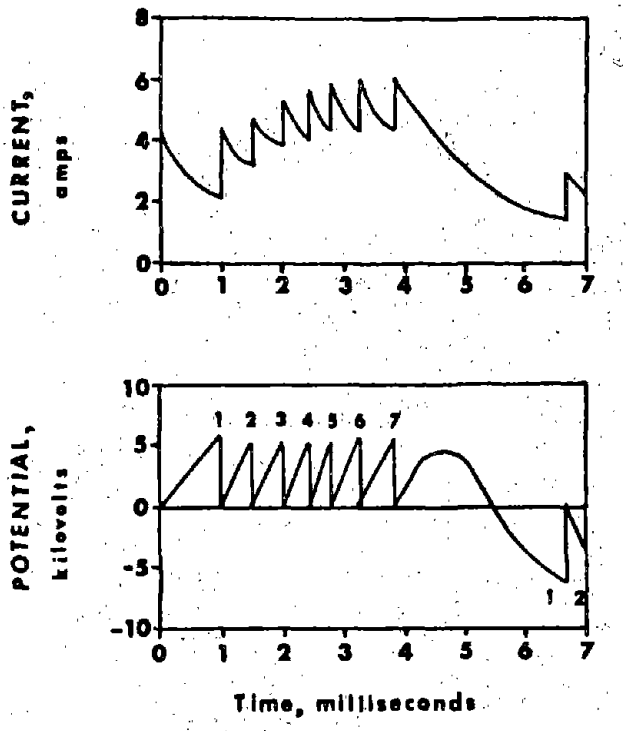

Figure 30 - Oscillograms Used for Calibration of A.C. Spark Energies

APPENDIX IV

Apparatus Effects on Equilibrium Flammability Envelopes

Rates of combustion are controlled by thermal processes or the nature of the predominant chemical reactions. In either case the apparatus strongly affects the flammability results. Before standardization of apparatus and procedure the effects of tube diameter, spark energy and ullage were investigated. These results are described in the following sections. It was on the basis of these data that the apparatus and procedures were standardized upon for establishing the equilibrium flammability envelopes. As a result of these tests, the standard apparatus finally consisted of the four-inch diameter combustion tube, the high energy a.c. spark of 20 joules per spark, and a ullage of 87.5%.

Tube Diameter - Two tube diameters were studied to confirm their relative effects on equilibrium flammability envelopes. The two tube diameters were one and four inches. These diameters were selected on the basis of their producing high and low wall effects. The high wall effect produced by the one-inch tube is demonstrated by the equilibrium flammability envelopes shown in figures 31 and 32. The flammability envelopes produced with the one-inch tube,

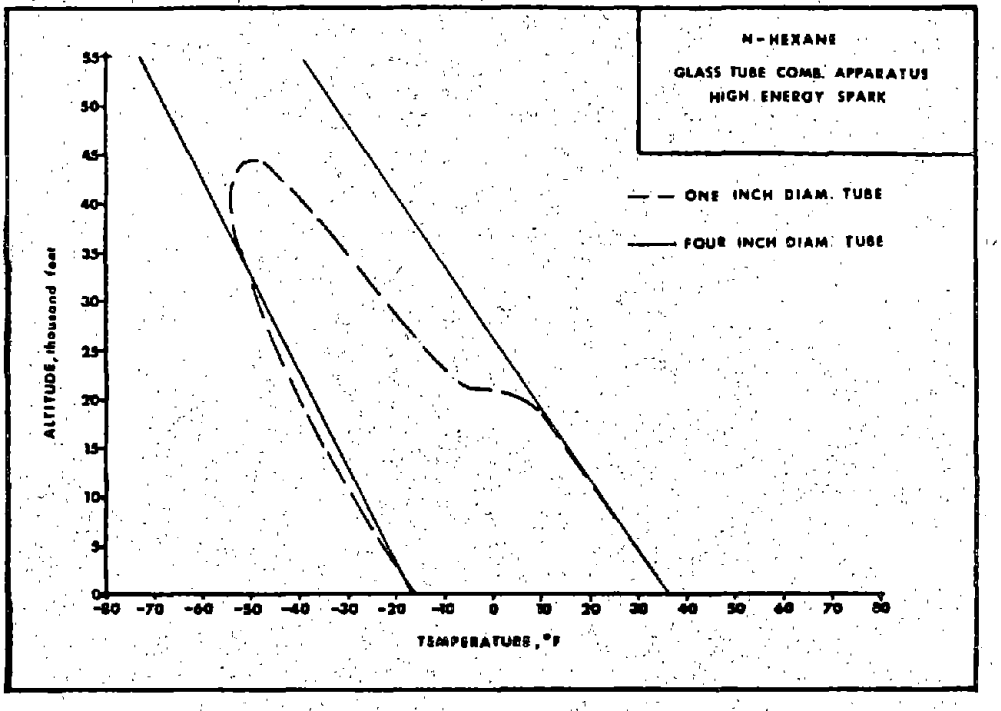

Figure 31 - Effect of Combustion Tube Diameter on n-Hexane Flammability

for both hexane and JP-4, are qualitatively quite similar. Unlike the four-inch tube data, which produced limits that were straight lines, the high wall effects of the one-inch tube produced curved limits with a plateau in the rich region as well as a limiting altitude at about 45,000 feet. With a four-inch tube, the wall effects were minimized and this became the standardized tube diameter.

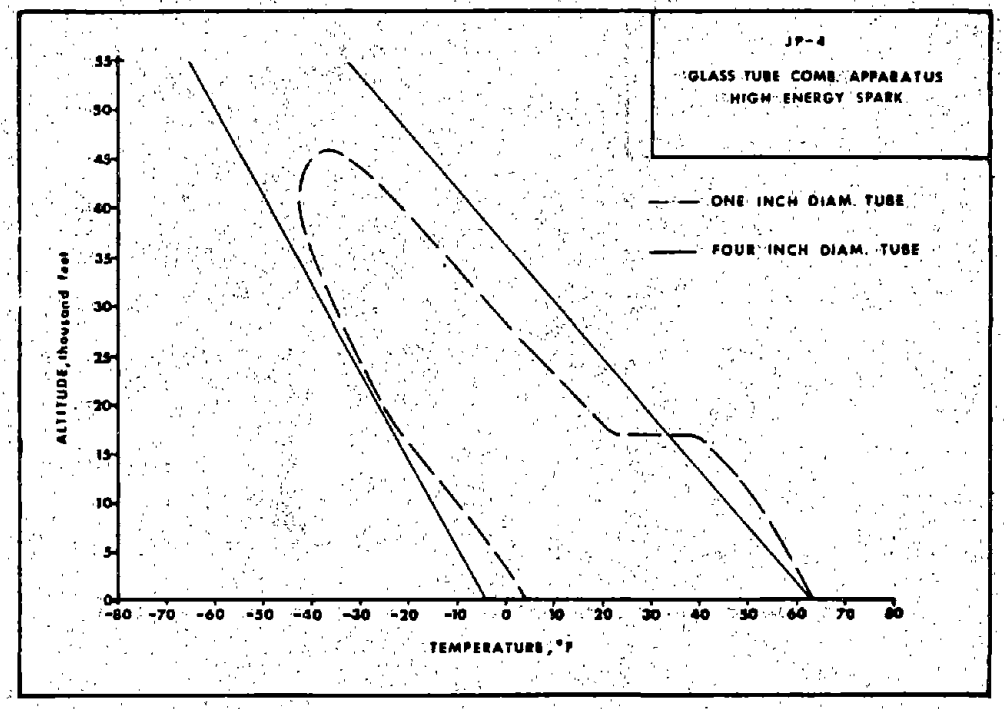

Figure 32 - Effect of Combustion Tube Diameter on JP-4 Flammability

Spark Energy - Two levels of spark energy were investigated to confirm their relative effects on equilibrium flammability envelopes. The high and low energy levels of 20 and 5 joules per spark were discussed in detail in Appendix III. The comparative effects of these spark energies on the flammability envelopes are shown in figures 33 and 34. The fuels used were Jet A-1 and Jet B, using the four-inch diameter combustion tube which produced minimum wall effects. In both figures it is shown that the low energy spark primarily affects the envelopes by narrowing the limits with respect to both temperature and altitude. There was no equivalent plateau at the rich limit as occurred with the one-inch tube.

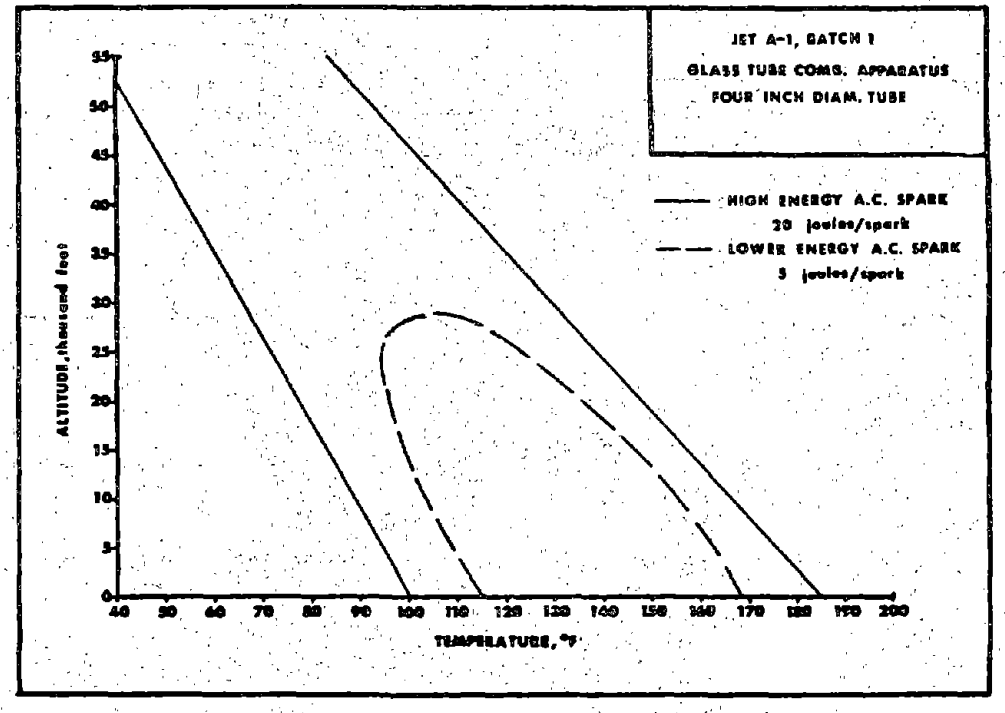

Figure 33 - Effect of Spark Energy on Jet A-1 Flammability

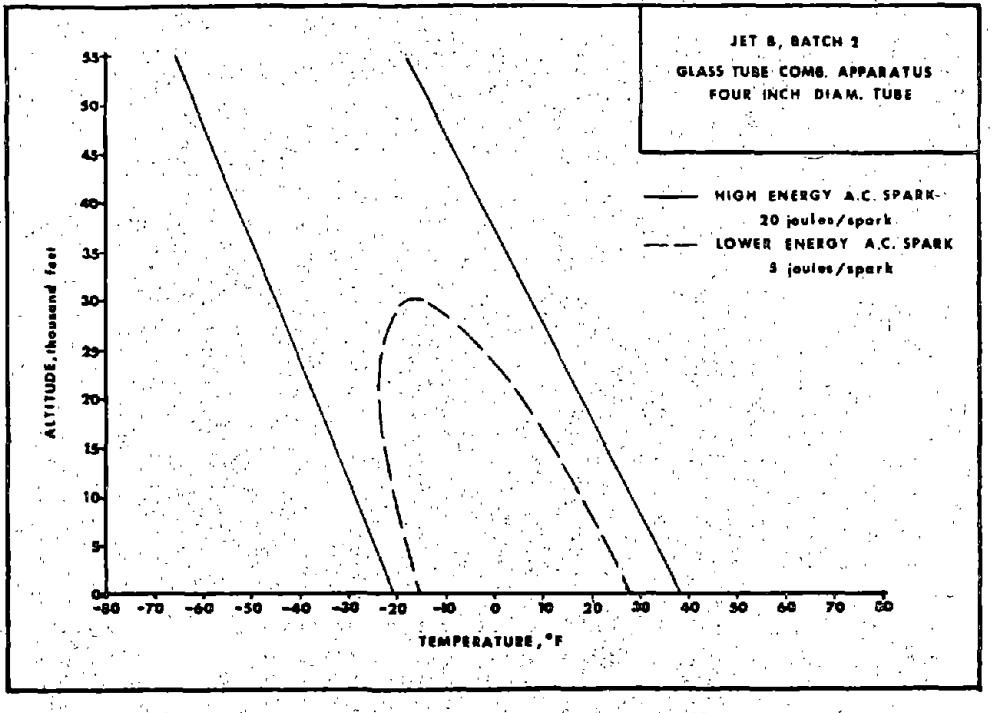

Figure 34 - Effect of Spark Energy on Jet B Flammability

Ullage - The relative unfilled volume of a vessel, expressed in terms of percent, is referred to as the ullage. The designed ullage of the combustion apparatus was 87.5%. This ullage was selected as it was similar to the ullage of the Reid vapor pressure apparatus. A selected number of flammability points were investigated at the higher ullage of 96.8%. The results indicated that the ullage of 96.8% was similar to the standard ullage of 87.5%. It was therefore concluded that there would be no adverse effects on the experimental data by standardizing upon the use of the 87.5% ullage.

Verification of Final Apparatus - An investigation was undertaken to establish the validity of the combustion apparatus, using the 4-inch diameter tube, high energy a.c. spark and associated procedures. This was accomplished by determining the equilibrium flammability limits for liquid n-hexane at sea level. The resulting data are shown in Table XII in comparison with the equivalent theoretical and experimental limits established by other investigators. The good agreement of these data validated the suitability of the apparatus and techniques.

TABLE XII

THE TEMPERATURES AT WHICH LIQUID n-HEXANE WILL FORM LIMITS OF FLAMMABILITY UNDER EQUILIBRIUM CONDITIONS

	Sea Level Flammability Limits, °F			
	Lean Limit		Rich Limit	
	Calculated	Experimental	Calculated	Experimental
Boeing (ref. 26)	-16	-20	+41	+43
Naval Res. Lab. (ref. 27)	-18	-	+41	-
AED *	-17	-17	+38	+36

* Glass Tube Comb. App; 4-inch diam. tube; High energy spark; 87.5% ullage

The repeatability as provided by both apparatus and method in determining the flammability limits was investigated using Jet A-1 as the fuel. The results are reported in Table XIII. With reference to this particular table, the flammability limit is defined as the mid-point between the nearest flammable and nonflammable point. The repeatability range of the limits at sea level, within the 95% level of confidence, was ±1.6°F for the lean limit and ±2.8°F for the rich limit. The repeatability decreased with increasing altitude as demonstrated for the rich limit range at 30,000 feet which was ±5.4°F.

TABLE XIII - REPEATABILITY OF THE EQUILIBRIUM FLAMMABILITY LIMITS

Fuel: Jet A-1, Batch 2 Ignition: High energy a.c. spark
Tube: 4 inch diameter Ullage: 87.5%

Sea Level Limits						30,000 Ft. Limit		
Lean Limit			Rich Limit			Rich Limit		
Flamm. Point °F	Non Flamm. Point °F	Est. Limit °F	Flamm. Point °F	Non Flamm. Point °F	Est. Limit °F	Flamm. Point °F	Non Flamm. Point °F	Est. Limit °F
90	85	87.5	163	167	165	115	121	118
92	85	88.5	163	169	166	118	124	121
92	86	89.0	166	169	167.5	120	124	122
92	86	89.0	166	169	167.5	121	125	123
93	86	89.5	165	170	167.5	123	128	125.5
93	86	89.5	166	172	169	117	122	119.5
Avg. of the Limits, °F		88.8			167.1			121.5
Std. Deviation of the Limits, °F		0.8			1.4			2.7
95% Confidence Limit Range		87 - 90°F			164 - 170°F			116 - 127°F

APPENDIX V

Calculation of the Flammability Limits of Fuels

General - A procedure is described herein for calculating the temperatures of the equilibrium lean and rich flammability limits of fuels at any given altitude. The method is based on the calculation of fuel/air ratios from empirical and theoretical relationships between measured distillation data, fuel vapor volumes and vapor pressures. It is assumed that the flammability limiting fuel/air ratios (on a weight basis) are constant with respect to pressure and temperature and are the same for all fuels. Conversion of fuel/air ratios from a weight to a volume basis is accomplished by estimating the molecular weight of the vapors. The correlations of Barnett and Hibbard (14) are used to determine the average molecular weight of the vaporized fuel from its 10% distillation temperature. At a given altitude, the vapor pressures required to produce the required fuel/air ratios are calculated by applying Dalton's Law of partial pressures. The equilibrium temperatures which will produce these vapor pressures are estimated by means of the Haas-Newton equation. Use of the latter equation was made possible by treating the fuel as a single component hydrocarbon having a boiling point represented by the 5% distillation temperature of the fuel.

Procedure - The calculation of the vapor pressure required to provide a given fuel/air ratio in a fuel tank is based on equation (1), which is an expression of Dalton's Law.

$$P_T = \left[\frac{\frac{W_F}{M_F} + \frac{W_A}{M_A}}{\frac{W_F}{M_F}} \right] P \qquad (1)$$

in which

W_F = weight of fuel vapor

W_A = weight of air

M_F = molecular weight of fuel vapor (figure 35)

M_A = molecular weight of air

P_T = total pressure in the tank, psia

P = vapor pressure of the fuel, psia

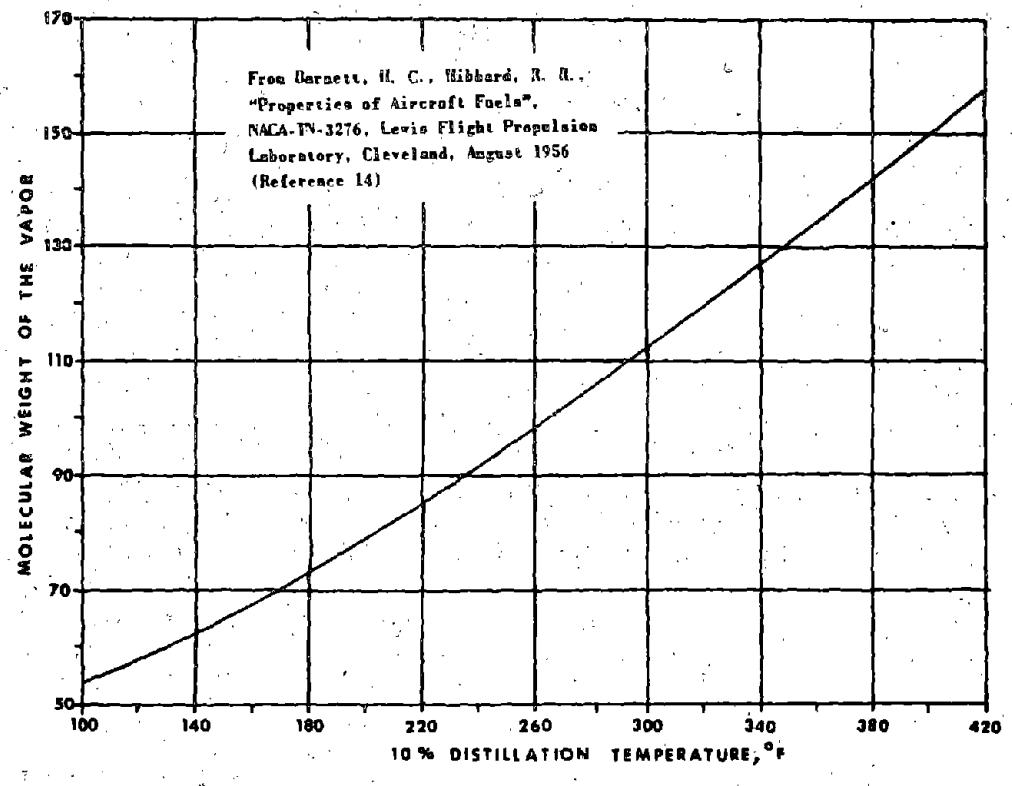

Figure 35 - Molecular Weight of Vaporized Fuel

By assuming weight fuel/air ratios of 0.035 for the lean limit and 0.28 for the rich limit, and inserting appropriate values in equation (1), the flammability limit vapor pressures can be expressed as follows:

$$P_L = P_T \left[\frac{52.05}{M_F + 1.0} \right] \qquad (2)$$

$$P_R = P_T \left[\frac{416.4}{M_F + 8.1} \right] \qquad (3)$$

where

P_L = Vapor pressure of the fuel required for the lean flammability limit, mm Hg abs.

P_R = Vapor pressure required for the rich limit, mm Hg abs.

P_T = Total pressure at the desired altitude, psia

M_F = Molecular weight of the fuel vapor

The equilibrium temperature of the system which will produce a given vapor pressure, and hence fuel/air ratio, is estimated by using the following form of the Haas-Newton equation (28).

$$T_2 = \frac{T_1 (0.15 \log P - \Phi - .43) - 273.1 \log P + 786.7}{1.15 \log P - \Phi - 3.31} \qquad (4)$$

where

T_1 = the normal boiling point of the fuel estimated as the 5% distillation temperature, °C

T_2 = temperature required to produce the desired fuel/air ratio, °C

P = vapor pressure of the fuel (equation (2) or (3)), mm Hg abs.

Φ = entropy of vaporization at T_1 and one atmosphere pressure (from figure 36)

When the resulting temperatures and respective pressure altitudes are plotted on a graph of altitude versus temperature, flammability envelopes are produced. These envelopes are bounded by straight line lean and rich limits similar to those obtained by use of the four-inch diameter glass tube with high energy spark.

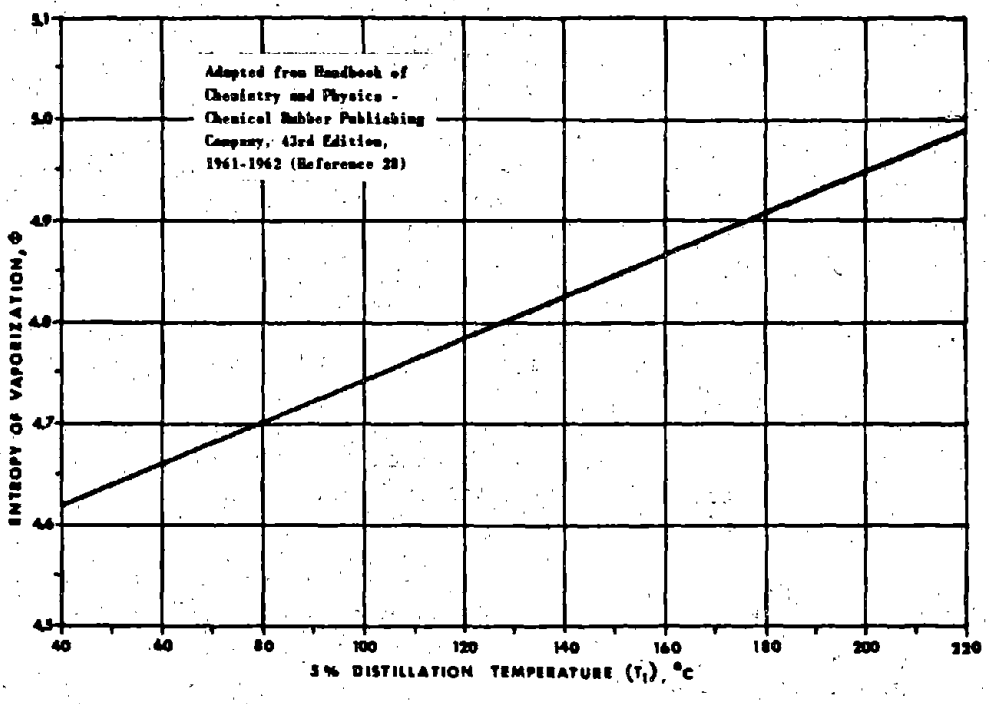

Figure 36 - Entropy of Vaporization for Hydrocarbon Fuels

APPENDIX VI

Fuel Slosh Tank Experiments

General - The presence of fuel spray or droplets in the vapor space was expected to have a marked effect on the characteristic equilibrium flammability limits. It was necessary to develop some insight into the manner in which aircraft dynamics affect fuel behavior to serve as a model for the flammability studies. A fuel slosh tank was constructed to permit the visual observation and photographic documentation of the effects of simulated aircraft dynamics on fuel. The information gained from these slosh tank studies proved to be invaluable in the design of the dynamic combustibility apparatus and formulating the experimental approaches utilized in defining the effects of dynamics on flammability limits.

Apparatus - The fuel slosh tank, shown in figure 37, was constructed to determine the effects of rocking and vibration on fuel sprays. The basic tank was constructed of 1/4 inch aluminum plate, welded to form a box, having the dimensions 12" x 12" x 36". The top and side windows were made of 1/2" thick plexiglass. To simulate internal wing tank members, baffles were constructed and placed equidistant at the bottom of the tank. Variable positions of the baffles were possible by making them removable. The baffles were held in place by vertical slots at the tank bottom. A maximum of five baffles could be utilized, each having the dimensions of 3" x 12". The vent line and fill valve were located at the same end of the tank. The vent also served as an inlet for nitrogen gas which was used to inert the vapor space. The tank was secured to a rocking table by adjustable turnbuckles, through the two rings welded at the tank ends. To preclude the possibility of fatigue failure of the retaining rings by the severe vibration, a frame was constructed, using steel "I" beams, which fitted over the tank top, clamping the tank to the rocking table. The table was an L.A.B. Rocker and Vibration Machine, Type 5670. This table was capable of producing various rocking and vibration frequencies individually or in combination.

Experimental Procedure - The rocking angle was kept constant throughout the program at ±15 degrees. Only two rocking rate levels were investigated, 5 and 25 cycles per minute. The vibration amplitude was kept constant throughout at ±1/8"; the vibration frequencies used were generally at three levels, 0, 12.5 and 15 cycles per second. Two baffle combinations were investigated where the distance separating the individual baffles were 6 inches and 18 inches. When no baffles were used, only the simulated bulkheads, (the tank ends) remained as an obstacle to fuel flow. Regardless of whether baffles were used or not, the bulkhead analog produced an

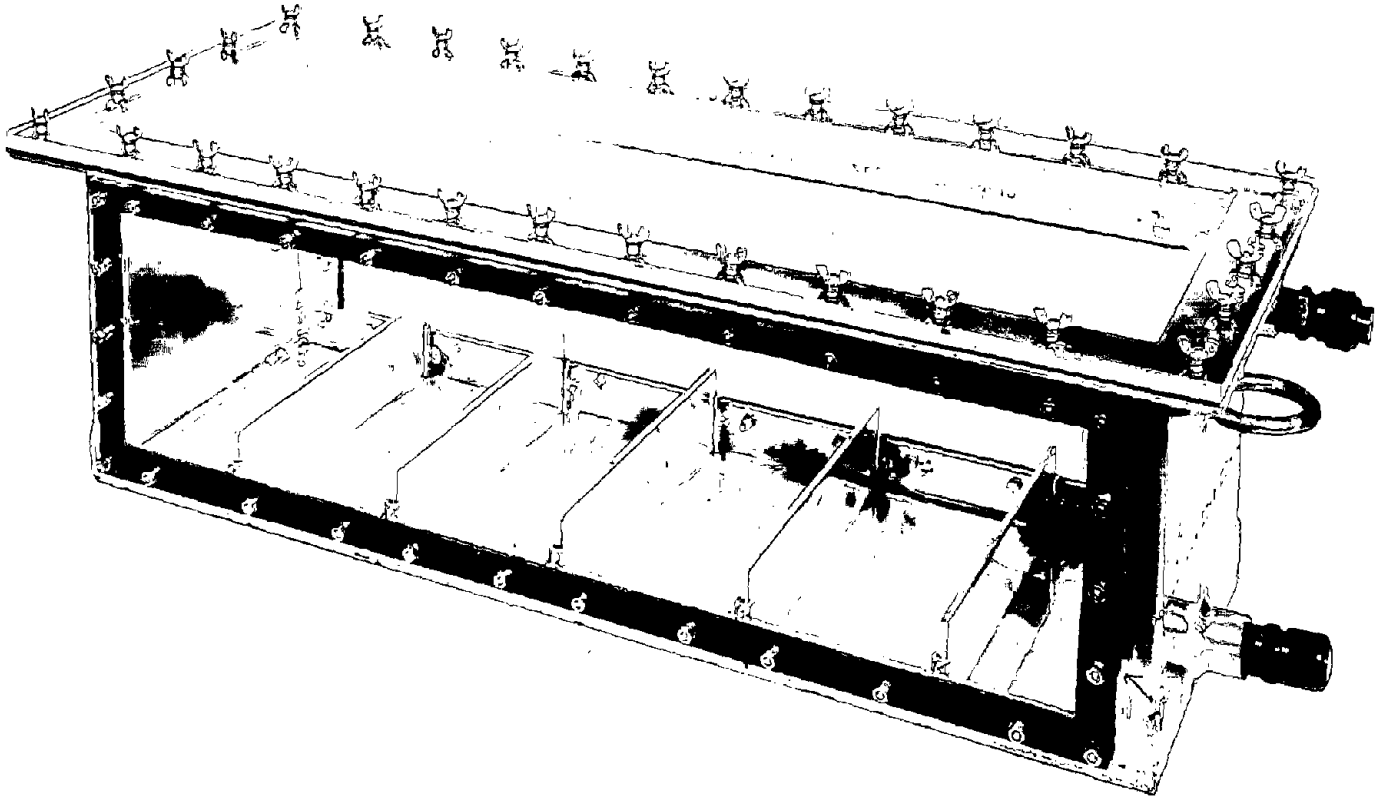

FUEL SLOSH TANK

PHOTO NO: CAN-370657(L)-8-65

FIGURE 37

PHOTOGRAPHIC DEPARTMENT
NAVAL AIR ENGINEERING CENTER
PHILADELPHIA 12, PA.

effect on the fuel that was a function of the relative rocking motion of the tank and fuel. As the tank rocked back and forth, the fuel would circle back over itself resembling a breaking ocean wave. This violent wave action at the tank ends is referred to throughout the report as a "high structural effect". During the rocking cycle, the condition when the tank was passing through the horizontal level is referred to as a "low structural effect".

High speed still photographs were taken of the tank at the various combinations of rocking rate, vibration frequencies and relative positions during the rocking cycle (the low structural effect being at 0° from the horizontal, and the high structural effect at ±15°). Exposure times of the photographs were 1/2800 of a second. From the photographs, the proportion of the tank ullage, in which the presence of spray could be discerned, was mapped out and reported as an estimate of the percentage of available vapor space containing spray.

Results - The data, representing the relative proportions of the tank ullage containing sprayed fuel, was statistically analyzed. The statistical analysis was based upon the principles used in the "analysis of variance". The results, showing the effects of the individual variables, without interaction, are shown in figure 38. The results can be summarized by stating that, within the range of conditions that were investigated, vibration was the most significant cause of spray. Rocking produces a lesser amount of spray than vibration. In addition, the rocking produces foam which in turn reduces the amount of spray produced by vibration. Because the rocking of JP-5 tended to produce more foam than JP-4, the data shows that spray is produced in greater quantity with the JP-4 fuel than with JP-5. The results with respect to structural effect, baffle number and tank ullage are inconsistent and appear not to be significant.

A pictorial representation of these conclusions is given in figure 39. The four photographs represent constant conditions of fuel height, vibration frequency and amplitude, baffle number and a low structural effect (the horizontal position during the rocking cycle). The variables are rocking rate and fuel. It can be seen that, as the rocking rate increases, going down in the individual columns, spray decreases. JP-4 fuel results in more spray than JP-5 fuel (going across the rows from left to right). Likewise, the JP-4 foams less than JP-5 under equivalent conditions.

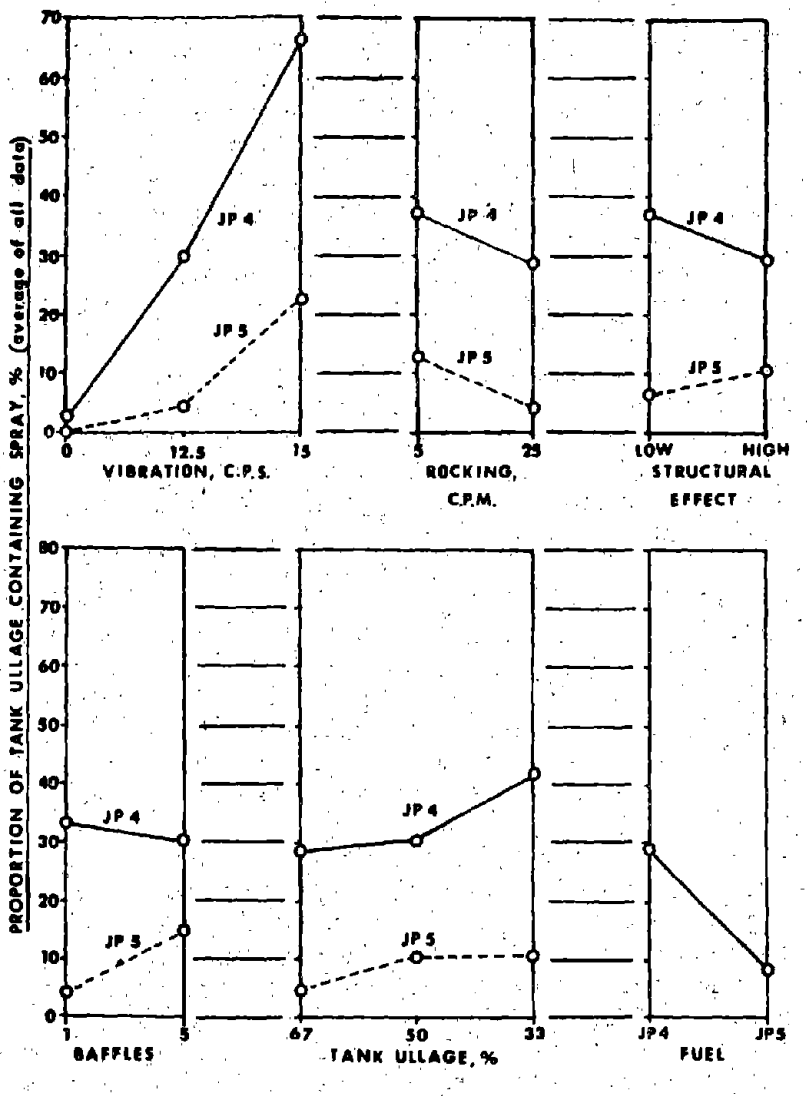

Figure 38 - Fuel Spraying by Simulated Aircraft Dynamics

NOT REPRODUCIBLE

Fuel: JP-4
Rocking Rate: 5 c.p.m.

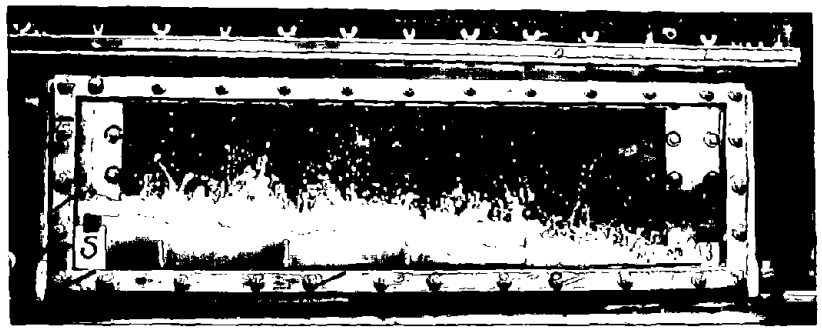

Fuel: JP-5
Rocking Rate: 5 c.p.m.

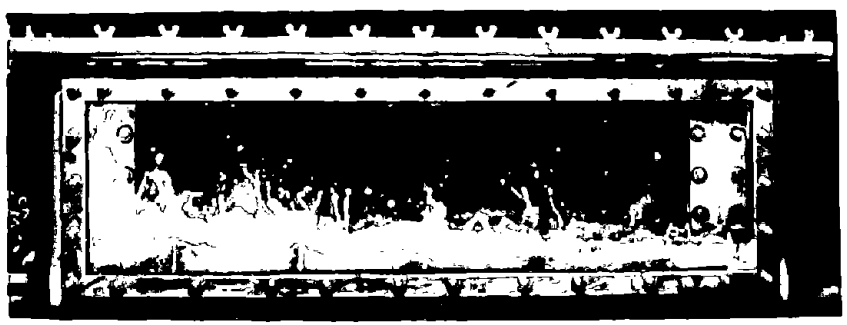

Fuel: JP-4
Rocking Rate: 25 c.p.m.

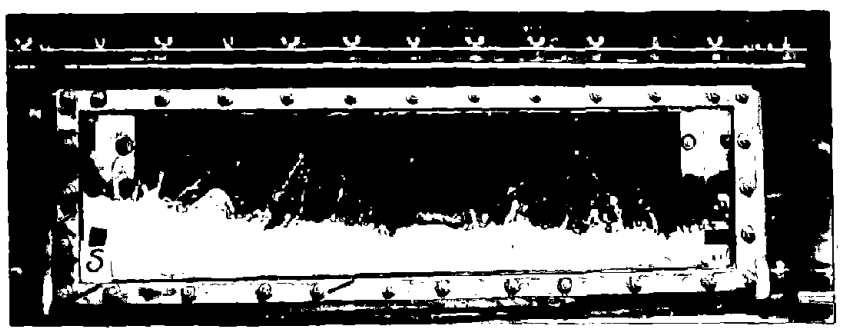

Fuel: JP-5
Rocking Rate: 25 c.p.m.

Fuel Height: 3 inches
Rocking Angle: ± 15 degrees
Vibration Amplitude: ± 1/8 inches
Vibration Rate: 15 c.p.s.
Baffle Number: 5
Structural Effect: Low

PHOTO NO: CAN-372222(L)-11-65

EFFECT OF ROCKING, VIBRATION AND FUEL TYPE ON SPRAY

FIGURE 39

APPENDIX VII

Dynamic Combustion Apparatus

General - The dynamic combustibility apparatus was designed to provide an instrumental description of flammability in terms of pressure and temperature transients, under both static and dynamic conditions. Vibration was the means by which dynamic motion was simulated.

Apparatus - The dynamic combustibility apparatus is shown schematically in figure 40. It consisted of a combustion bomb mounted in a temperature control chamber. By means of an extension to an electromagnetic shaker, combustion could be studied under vibrating conditions in addition to the static state. The combustion bomb was made by modifying a surplus 2½ gallon aircraft hydraulic accumulator, having the approximate dimensions of 9 inches in diameter and 15 inches in height with a burst strength of 3000 psi. To the accumulator, three ports were welded: the left port on the bomb was for light beam entrance into the chamber; the port at the right, in direct opposition to the light beam entrance, held a photocell for measuring the transmitted light. The port at the center, which was at right angles to the incident light beam, also held a photocell, which measured scattered light. Any appearance of spray or mists in the path of the transmitted light photocell resulted in a reduction of photocell output; and concurrently, spray caused an increase in the photocell output measuring the scattered light. The photocells were designed to withstand high pressure transients. Details of construction for the photocell was shown in figure 41. The plexiglass windows were recessed in 1.2 inch diameter ports and were not damaged by the reactions. The two photocell outputs were recorded by strip chart recorders. The light source used was a common 50 watt incandescent bulb contained in a standard explosion-proof reflector housing mounted in the environmental chamber opposite the window port. Bisecting the angle between the photocell ports, an igniter plug was located so the spark was located at the intersection of the scattered and transmitted light paths. The igniter plug was the same as that used for J-57 turbine engines. The power supply for the igniter plug was a General Laboratory Associates Exciter, P/N 40355. This GLA Exciter is a capacitor discharge electronic ignition system which is used to start turbojet and turboprop aircraft engines. In conjunction with the J57 igniter plug, the system provided an ignition energy in the range of 16 to 24 joules per spark. This range is the nominal value as rated by the manufacturer, and is of comparable intensity on a per spark basis to the "high" energy ignition as used with the glass tube apparatus.

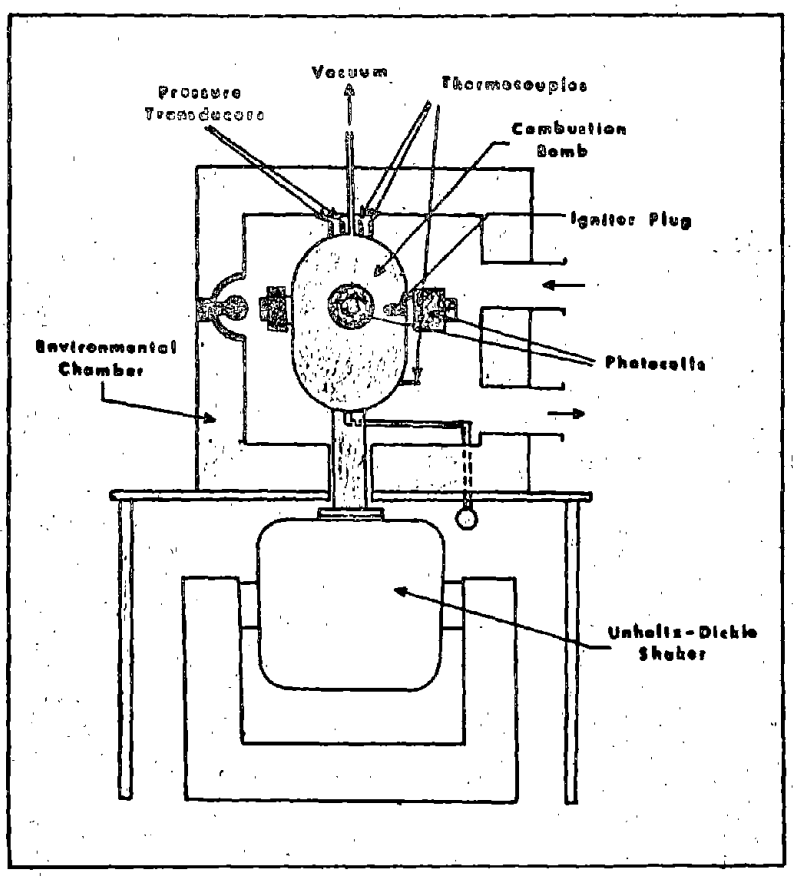

Figure 40 - Dynamic Combustion Apparatus

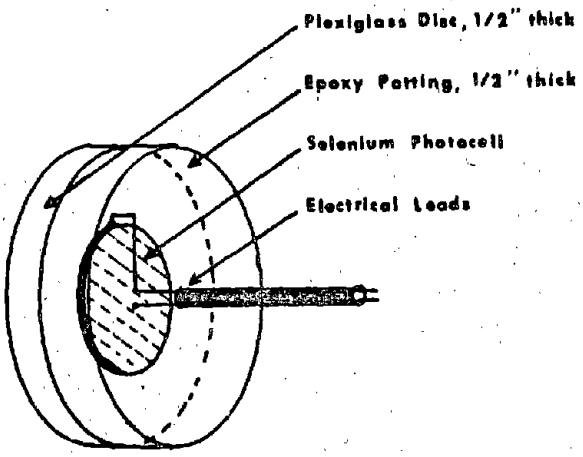

Figure 41 - Photocell Used with the Dynamic Combustion Apparatus

Three thermocouples were installed in the combustion bomb. Two of the thermocouples measured the steady state temperatures of the vapor space and fuel using a Brown Indicator as the temperature readout. The third thermocouple was recorded on one channel of a dual trace oscilloscope which was used to determine the transient temperature rise in the vapor space, occurring at ignition. In addition to the three thermocouples, the combustion bomb was instrumented with two pressure transducers. One pressure transducer, a Statham 0 to 100 p.s.i.a. transducer, was used to monitor steady state pressures. Its output was recorded on a strip recorder. The second pressure transducer, a Statham flush diaphragm type transducer of 0 to 300 p.s.i.a., monitored the pressure transients occurring at combustion via the second channel of the dual trace oscilloscope. At the base of the combustion bomb, a fuel-fill-and-drain valve was located. In conjunction with the top vacuum line, the fuel-fill-and-drain valve permitted experimental altitude simulation in a manner similar to that described for the glass tube combustion apparatus. The Unholtz-Dickie Shaker was used to vibrate the combustion bomb within the environmental chamber. The shaker was capable of providing frequencies ranging from 0 to 20 cps and amplitudes from 0 to ±1/8 inches. Vibration settings were conveniently controlled by means of a console control, as all vibratory motion was electromagnetically induced by the shaker.

Experimental Procedure - The basic principle for charging the bomb was similar to that described for the glass tube apparatus. The combustor was first purged of all combustible material, then the air was evacuated with the vacuum pump to a vacuum of 29 to 29.5 inches of mercury. With the vacuum pump off and the valves closed, the vacuum was retained by the bomb. By virtue of the existent negative pressure in the combustion bomb, the fuel, 1.18 liters, was drawn up through the fuel-fill-and-drain valve. This standardized fuel volume produced a system ullage of 87.5% which was identical to the ullage used in the glass tube experiments. Fuel temperature was stabilized at the experimental temperature. The pressure was then increased to the desired altitude equivalent by a dry air bleed through the fuel-air-and-drain connection. From this point on, the similarity between the dynamic and glass tube apparatus techniques diverged. The apparatus was shaken at a frequency of 15 cps and an amplitude of ±1/8 inches, which produced a violent rain of sprayed fuel within the vapor space. Ten minutes was allowed for the scrubbing of the air by the fuel and an additional ten minute period was allowed for settling. A photocell confirmation was made showing that a suspension of fuel did not persist in the vapor space. Without a doubt, this technique of air scrubbing certainly did saturate the air with fuel, and so resulted in equilibrium.

Having established an equilibrium fuel/air relationship, flammability experiments were conducted within three basic parameters:

a. Static conditions representing equilibrium.

b. Dynamic conditions where spray droplets existed but were not in the vicinity of the ignition source as established by prior optical calibration. This was produced as follows:

Vibration amplitude:	±1/16 inches
Vibration frequency:	10 cps
Fuel Volume:	1.18 liters
Fuel to Spark:	5.5 inches
Spray to Spark:	≥1.8 inches
Ullage:	87.5%

c. Dynamic conditions where spray droplets completely surround the ignition source. This state was produced as follows:

Vibration amplitude:	±1/8 inches
Vibration frequency:	15 cps
Fuel Volume:	1.18 liters
Fuel to Spark:	5.5 inches
Spray to Spark:	0 inches
Ullage:	87.5%

A major distinction between the dynamic combustibility apparatus and the glass tube apparatus resulted in defining a flammable point. The convenient definition by visual observation was no longer applicable to the dynamic apparatus. Instead, as a substitute, instrumental definitions were applied, which provided a convenient frame of reference for data evaluation. For the dynamic apparatus, the ignition responses were assigned to the following categories:

a. High Reaction: any ignition point which had a pressure rise greater than 4 psi and/or temperature rise greater than 50°F.

b. Low Reaction: any ignition point which had a pressure rise less than 4 psi and a temperature rise less than 50°F.

c. No Reaction.

APPENDIX VIII

Mists in Aircraft Fuel Tanks

During the course of studies involving aircraft dynamics, it was observed that as the pressure is reduced in a fuel tank, mists suddenly appear in the vapor space. Upon continued reduction of the pressure, the mist would cease to form and then finally disappear. Since this reduced pressure is analogous to an ascending aircraft, similar mists must necessarily be formed in the fuel tanks. Upon searching the literature, no reports or reference to this phenomenon could be found. Investigations were initiated to develop insight into the formation of such mists and the manner in which they could influence the combustibility envelopes.

The possibility that these mists were produced either by water in the fuel or in the air was eliminated by the following experiment. Pure, dry, n-hexane was substituted as the fuel. Dissolved water in the hexane had been removed by passing it through a column of silica gel. All air in the vapor space was dry. With this system, even though moisture was absent, dense mists still appeared. The fact that mists could be produced, in the absence of water, evidenced the fact that another mechanism was responsible.

Another proposed explanation for this particular type of misting suggested that the expansion of the gas by reducing the pressure also reduced the temperature, causing condensation to occur, i.e. Joule-Thomson effect. The logic used in this argument was that the temperature of the vapor is reduced below the dew point. This argument was not pursued further as the analogy of this system to the Joule-Thomson effect is not a valid one. In our particular system, the pressure is reduced slowly, not by rapid expansion of the gas through a throttle. Secondly, the tank was not insulated. Some heat exchange occurred with the surrounding atmosphere, and therefore, the experimental conditions tended to be more isothermal than adiabatic. Thirdly, since less than one atmosphere was the maximum pressure differential produced, the Joule-Thomson effect, even if applicable, at best could only have produced, under adiabatic conditions, a temperature change that would be no greater than a fraction of a degree.

An interesting characteristic of this mist was noted. If the tank were first agitated and then held motionless for a ten minute period (which was quite adequate for settling visible suspended droplets) copious quantities of mist would appear upon reducing the pressure. However, when the tank was left standing overnight, no mist would form, even at extremely high rates of pressure reduction.

Mist would form only if the liquid or air were disturbed prior to pressure reduction. This strongly suggests that the agitation produced the necessary nucleation sites required for the growth of the mist droplets. These nucleation sites are most likely polymolecular, behaving as a gas but smaller in size than can be visually confirmed by the Tyndall effect. However, with extended periods of settling, a vapor space condition was produced, which lacked adequate nucleation sites.

From high speed movies of the vapor space, using dark field illumination, it was revealed that the mist forms simultaneously throughout the vapor space. The concentration of the mist, immediately on forming, appeared to be somewhat uniform throughout the tank. That the mist formed uniformly and simultaneously at the top of the tank which was 9 inches from the surface, as compared to a point which was immediately above the liquid, supported the conclusion that the mist is produced by the existent fuel present in the air as a vapor. The mist droplets appeared to be quite stable and showed no tendency to disappear by evaporation. The mist disappeared primarily by settling.

A series of fuel misting experiments was introduced to study some of the parameters influencing mist formation. The mist concentration was measured by photocells recording the intensity of scattered light produced, using the technique of dark field illumination. Some typical optical measurements, which are in reality a measure of mist concentration, are shown in figure 42 as they were recorded at four different climb rates: 1400 ft/min, 3700 ft/min, 5900 ft/min, and 10,600 ft/min. Included in the same figure are the two different fuel types: JP-4 representing the wide-cut fuel, and Jet A, representing aviation kerosene. From these curves, certain conclusions can be drawn concerning mist formations of fuel:

a. The greater the altitude ascent rate, the greater the formation of mists.

b. JP-4 fuel produces more mist than Jet A.

c. The mists, produced by Jet A, appear to be more persistent than those of JP-4.

An additional comparison was made between the two fuels by plotting the maximum recorded mist values against the corresponding altitude ascent rate. These data are shown in figure 43 comparing JP-4 and Jet A. This figure suggests that the wide-cut, JP-4, tends to produce twice as much mist as the aviation kerosene, Jet A.

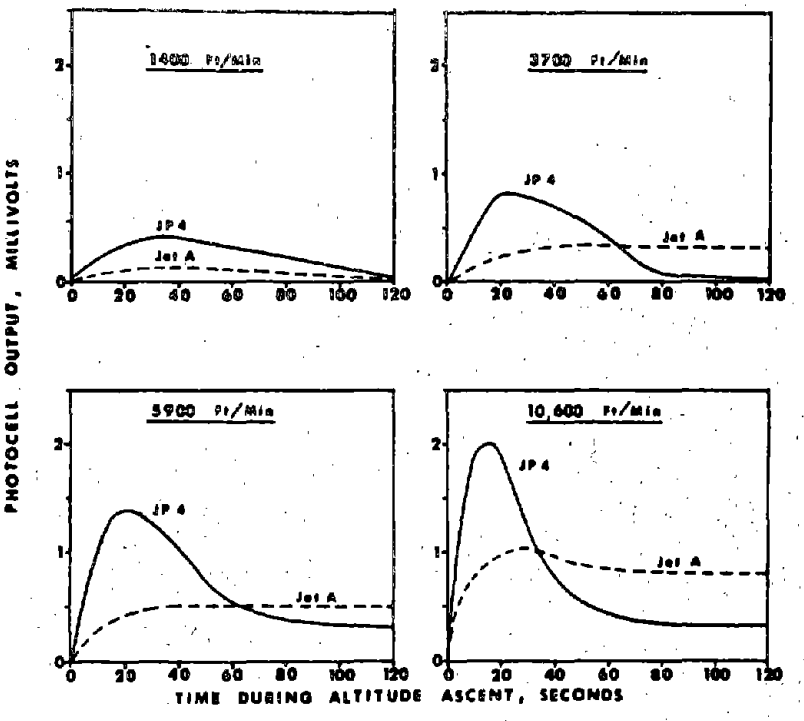

Figure 42 - Typical Misting Data Obtained at Several Climb Rates

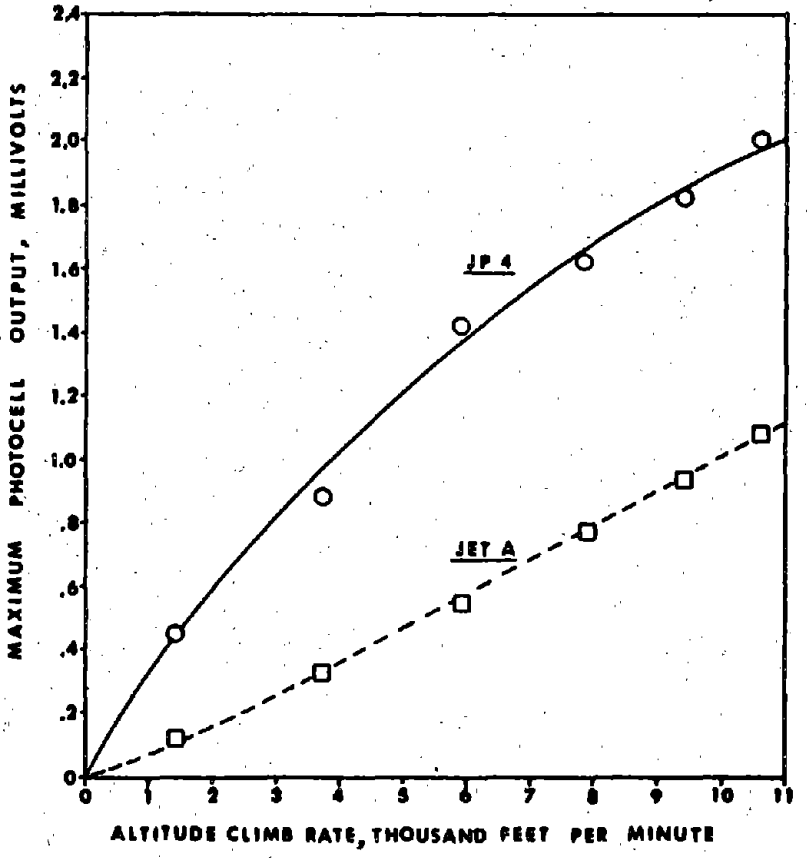

Figure 43 - Misting as a Function of Climb Rates